# The Annual Cycle and Interannual Variability in the Tropical Pacific and Indian Ocean Regions*

GERALD A. MEEHL

*National Center for Atmospheric Research,** Boulder, CO 80307*

(Manuscript received 15 April 1986, in final form 27 June 1986)

ABSTRACT

The annual cycle of outgoing longwave radiation (OLR), clouds, precipitation and sea level pressure is studied from satellite and station data in the tropical Indian and Pacific sectors. A region of heavy convection, termed the tropical convective maximum, moves from north to south and west to east in the Indian and Pacific sectors as the mean annual cycle proceeds from northern summer to northern winter. During its return excursion northwestward from northern winter to northern summer in the Indian sector, it is not as strong as in the preceding half of the annual cycle. To study interannual fluctuations of the annual cycle in these regions, Indian monsoon rainfall is chosen as an indicator of precipitation and convection in the summer monsoon region. Relatively strong and weak years of monsoon rainfall are selected and used as a starting point to follow the evolution of the annual cycle in the two sets of years. More than two-thirds of the monsoon seasons since 1900 are classified as either relatively strong or weak indicative of the biennial tendency of monsoon rainfall. Examination of sea level pressure, precipitation, and sea surface temperatures shows the dynamically coupled ocean–atmosphere system in the Indian–Pacific region to be involved with producing Southern Oscillation-type signals in atmosphere and ocean in these sets of years, with extremes in the system being manifested as Warm and Cold Events. This is associated with the alternate strengthening and weakening of the mean west-to-east exchange of mass from the Indian to Pacific sectors in the atmosphere, and the interactive response of the ocean in helping reinforce and maintain those anomalies. For example, a year with a relatively strong Indian monsoon is characterized by lower pressure, warmer SSTs, and greater precipitation to the west of the South Pacific Convergence Zone (SPCZ) ahead of the convective maximum as it moves southeastward with the seasonal cycle from northern summer to northern winter. At the same time, higher pressure, decreased precipitation and low SSTs are in evidence to the east of the SPCZ in the tropical Pacific. In the extratropics, a weakened circumpolar trough in the Southern Hemisphere midlatitudes during May–July south of New Zealand and southwest of Australia is associated with strong subtropical highs in the Indian and Pacific oceans. A relatively weak year is characterized by opposite conditions through the course of the annual cycle. A transition from strong to weak is made in northern spring, as low SLP and warm SST in the SPCZ area are associated with westerly wind anomalies in the equatorial western Pacific and a weakened South Pacific High. Warm SSTs then become established in the tropical eastern Pacific as a result of the dynamic response of the ocean, and a weak year begins. Since the system is not purely biennial, such transitions do not happen every year. Extremes in this oscillation, the Warm and Cold Events associated with the Southern Oscillation, happen less frequently and the anomaly patterns are of much greater amplitude than strong and weak years without Warm and Cold Events. Similar, albeit weaker, patterns are still in evidence throughout the composite annual cycles of these other years. These results point out that processes in the Indian–Pacific region are continually evolving from one annual cycle to the next and that Warm and Cold Events are not discrete occurrences but are extremes of patterns which appear in many other years as part of the dynamically coupled air–sea system in this region.

## 1. Introduction

The annual cycle of convection in the tropical Indian and Pacific Oceans has been widely studied for many years to attempt to explain interannual variation. Walker (1923, 1924) documented statistical relationships between those regions. Bjerknes (1969) introduced the term "Walker Circulation" to describe large-scale west–east circulations between the western and eastern tropical Pacific associated with regional centers of organized convective activity. Krishnamurti (1971) and Krishnamurti et al. (1973) showed that the Walker circulation in the Pacific was part of a much larger regime of east–west circulations in the global tropics.

The interannual variations in the exchange of mass between the Indian and Pacific Oceans has been termed the Southern Oscillation (e.g., Walker and Bliss, 1930). The Southern Oscillation (SO) has been linked to variations of sea surface temperatures (SSTs) in the tropical Pacific (e.g., Bjerknes, 1969) referred to as El Niños, El Niño–Southern Oscillation Events, or Warm Events (e.g., van Loon and Madden, 1981; Rasmusson and Carpenter, 1982). During these periods the normal

* A portion of this study is supported by the U.S. Department of Energy as part of its Carbon Dioxide Research Program.

** The National Center for Atmospheric Research is sponsored by the National Science Foundation.

west-to-east circulation between the Indian and Pacific is weakened and anomalous heavy convection and high SSTs in the tropical Pacific tend to be associated with suppressed convection in the monsoons over southern Asia. This is often manifested by a decrease in precipitation in the Indian monsoon (e.g., Pant and Parthasarathy, 1981; Rasmusson and Carpenter, 1983; Mooley and Parthasarathy, 1983; Khandekar and Neralla, 1984) as well as in the Southeast Asian or Australian monsoon (e.g., Tanaka, 1981; Allan, 1983). However, these relationships are based mainly on correlation studies which have some inherent problems which must be kept in mind (e.g., Ramage, 1983). So-called Cold Events in the tropical Pacific (van Loon and Shea, 1985) have been shown to be the complement of the Warm Events as the opposite extreme of the SO in the tropical Pacific.

The tropics, of course, do not act independently of influences from higher latitudes. The subtropical highs are linked to tropical convective activity via the north–south Hadley circulation in the southern Indian and Pacific Oceans (see schematic diagram in Meehl, 1987). The subtropical high in the southern Indian Ocean has been shown to be associated with activity in the Indian monsoon (Krishnamurti and Bhalme, 1976; Kuettner and Unninayar, 1982; Cadet, 1983). Onset of the Australian monsoon has been studied in the context of activity in the southern subtropics as well (Davidson et al., 1983). The South Pacific High and circulation in the subtropics of the western Pacific have been postulated to play a role in the formation of Warm and Cold events in the tropical Pacific (e.g., Keen, 1982; van Loon, 1984; Harrison, 1984; van Loon and Shea, 1985). Cold surges of midlatitude origin also have been linked to convective activity in the Southeast Asian region (Lau et al., 1983), in the tropical Pacific (Reiter, 1983), and in the northern Australian region (Love, 1985).

A dominant semiannual or twice-yearly oscillation in the position and intensity of the circumpolar trough of low pressure surrounding Antarctica is a well-documented feature of Southern Hemisphere mid- and high-latitude circulation. A comprehensive summary is given by van Loon et al. (1972). The circumpolar trough moves equatorward and weakens in southern winter and summer, and contracts and intensifies in southern spring and fall (van Loon, 1967). The months when the circumpolar trough is farthest equatorward, in June and December (van Loon and Rogers, 1984), are also the months of the onset of the Indian and Australasian monsoons, respectively (e.g., Kuettner and Unninayar, 1982; Nicholls et al., 1982; Davidson et al., 1983). This would suggest, along with the previously mentioned association of the subtropical highs and tropical convective activity, that the Southern Hemisphere midlatitude circulation may be related to the annual cycle and interannual variability in the tropics, and vice versa.

As Bjerknes (1969) originally suggested, ocean dynamics and associated sea surface temperatures play a critical role in this coupled air–sea system. Wyrtki (1975) hypothesized that a remote dynamical response in the tropical Pacific could be triggered by alterations of the trade winds. More recently ocean models have been used which are able to simulate many of the oceanic features of observed Warm Events. For example, Busalacchi and O'Brien (1981) and Cane and Zebiak (1985) have used idealized air–sea models to successfully simulate features which resemble observed Warm Events. Philander and Seigel (1985) have been able to trace the evolution of the 1982–83 Warm Event using the observed surface wind field with a fairly detailed Pacific Basin ocean model. An atmospheric GCM coupled to a simple slab ocean 50 m deep (Washington and Meehl, 1984) has been shown to produce SST anomalies as a consequence of omitting ocean dynamics which alter atmospheric east–west circulations to resemble anomalies observed during Pacific Warm Events (Meehl and Washington, 1985, 1986).

The purpose of this paper is to examine the observed behavior of the coupled air–sea system in the India–Pacific region first in terms of the mean annual cycle, and then in terms of year-to-year fluctuations of the system. Data sources will be reviewed in section 2, then the long-term mean annual cycle in the India–Pacific region will be examined in section 3 in terms of satellite and station data. Interannual variations will be addressed in section 4 using a long-term record of Indian monsoon rainfall as a starting point. An analysis of sea surface temperatures will be shown in section 5. Outgoing longwave radiation data will be analyzed in section 6. Relations to the midlatitudes of the Southern Hemisphere will be studied in section 7, and a discussion and conclusions will follow in section 8.

## 2. Data

The data used in this study to infer convective activity in the tropics is monthly mean outgoing longwave radiation (OLR). Changes of OLR have been used to study relative fluctuations of deep convection and implied rainfall in various tropical regions (e.g., Liebmann and Hartmann, 1982; Lau and Chan, 1983a,b; Weickmann et al., 1985). A detailed description of the outgoing longwave radiation data is provided by Gruber and Krueger (1984). They document differences in satellites and equatorial crossing times for the period in the present study from 1974 to 1982. These inhomogeneities are usually dealt with by using daily averages of the data and studying only monthly and annual timescales (Lau and Chan, 1983a,b). The OLR data in the present study are monthly means of daily averages provided by B. Briegleb of NCAR. The data are on a $2.5° \times 2.5°$ grid, and cover the period from June 1974–August 1982 with a gap from March to December 1978.

Two other datasets are used to compare with the long-term (8-year) monthly means of OLR. One is long-term monthly mean precipitation data from Jaeger (1976) digitized on a 4° × 5° global grid. The other is a set of long-term (8-year) monthly mean fractional cloud amounts compiled from gridded tropical neph-analysis data described by Sadler (1970). The period of record is from February 1966 to July 1973, and the data are digitized on a 2.5° × 2.5° grid from 27.5°S to 30°N. Sea surface temperature data from COADS are global marine data from 1854 to 1979 taken mainly from ships-of-opportunity. The data have been interpolated to a 2.5° grid as described by van Loon and Shea (1985).

The gridded Australian and South African analyses of sea level pressure (SLP) are used in addition to individual station data. The Australian data consist of monthly mean SLP on a 5° × 5° grid for the period April 1972 to May 1984 covering 10° to 85°S. The South African data are on the same grid and cover the period from January 1951 to December 1958.

## 3. The annual cycle in the tropical Indian and Pacific Oceans

The convective maximum generally associated with the Intertropical Convergence Zone (ITCZ) in the tropics is often perceived to move from north to south and back following the annual cycle of solar forcing as the sun crosses the equator twice each year. However, the distribution of land and sea alter the circulation in such a way that this is not strictly the case over the tropical Indian and Pacific. In fact, the geography in these regions dictates that the regional convective maximum moves not only meridionally but zonally as well in the Indian–Australian area. This movement has been noted, for example, by Lau and Chan (1983b). In the Pacific the ITCZ lies mostly north of the equator year round, and convective activity and rainfall south of the equator is generally associated with the SPCZ (e.g., see rainfall values in Jaeger, 1976).

In Fig. 1, eight-year monthly means of OLR are shown starting with northern summer in July and moving through the year for October, January and April. Units are W $m^{-2}$, and coldest areas below 220 W $m^{-2}$ are stippled to denote the strongest tropical convection. The dominant convective activity in the northern tropics in the Indian and Pacific sectors takes place in southern Asia during northern summer in July (Fig. 1a) in the midst of the monsoon season. Of somewhat less intensity, the ITCZ nonetheless is strong just north of the equator all across the Pacific. In October (Fig. 1b) the convective maximum in the Indian sector has moved south and east and activity in the ITCZ in the Pacific has begun to wane. By January (Fig. 1C) the heaviest convection has moved further south and east and has become established over Indonesia and northern Australia during the Australian monsoon season. The ITCZ north of the equator in the Pacific is weakest at that time of year, but convective activity in the South Pacific Convergence Zone (SPCZ), which extends diagonally from New Guinea southeastward into the Southern Hemisphere, is strongest at this time of year. Finally in April (Fig. 1d), the SPCZ has weakened but convective activity in the ITCZ in the eastern Pacific has begun to pick up.

An analysis of standard deviations (not shown) associated with the OLR values in Fig. 1 reveals great variability in the tropical Pacific in the region of the ITCZ and SPCZ. This has also been shown by Heddinghaus and Krueger (1981) for OLR from a shorter period. Therefore it must be kept in mind that the mean values shown in Fig. 1 include pronounced interannual shifts in intensity and position of the SPCZ, and in activity in the ITCZ.

To describe the meridional movement of the convective maximum in the Indian and Pacific sectors, annual cycles of zonal means covering 45° to 155°E and 155°E to 90°W are computed for OLR, precipitation and cloud cover data described earlier. The results in Fig. 2 are the annual average zonal mean for each latitude subtracted from the zonal mean for each month. As in Fig. 1, the annual cycle is depicted to start with northern summer and run through the year from May to the following April. In spite of the different data sources and periods, all three datasets show what was noted in the geographic plots of OLR in Fig. 1. In both sectors, a relative convective maximum (stippled area) lies north of the equator in July–August, and south of the equator in January–April roughly following the annual course of the sun. In the Indian sector this reflects the movement of active convection from the Indian monsoon north of the equator in northern summer to the Australian monsoon mostly south of the equator in northern winter. This can be seen in the geographical plots in Fig. 1. In the Pacific sector, it was noted in Fig. 1 that the ITCZ in the tropical Pacific lies mostly north of the equator year round, and in spite of large interannual variability, appears most active in the long-term means during northern summer. The maximum south of the equator during northern winter in the mean in Fig. 2b, d, and *f* is mainly due to activity in the SPCZ noted in Fig. 1 in the western Pacific. In this regard the north–south movement of the convective maximum in zonal means for the Indian and Pacific sectors is quite different.

To illustrate the zonal movement of the convective maximum, the same three datasets are used to compute annual cycles of meridional means. For each month and longitude, values are averaged along each longitude across the tropical band from 30°N to 30°S, covering the Indian and Pacific regions from 45°E to 95°W. These latitudinal limits are chosen to include most of the convective activity shown in Fig. 1 ranging from the Indian monsoon in the north to the SPCZ in the south. The results in Fig. 3 are the annual average me-

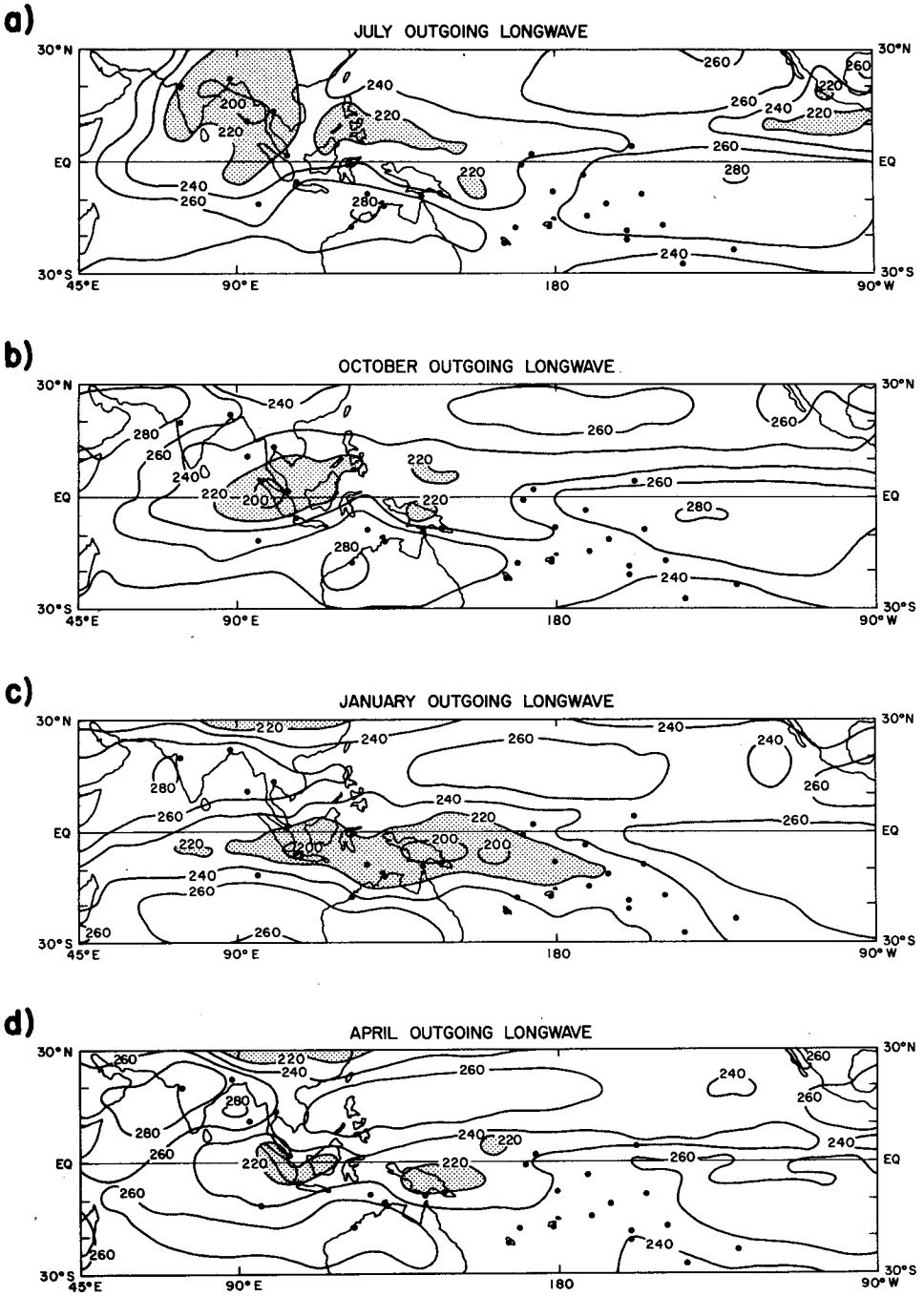


FIG. 1. Long-term means (eight years) of outgoing longwave radiation (W $m^{-2}$) for the period covering June 1974–November 1983 (1978 missing), for the Indian and Pacific sectors for (a) July, (b) October, (c) January, (d) April (after Janowiak et al., 1985). Areas less than 220 W $m^{-2}$ are stippled indicating greatest tropical convection. Dots indicate location of stations listed in Table 1. Stations are labeled for reference in Figs. 7–8.

ridional means for each longitude subtracted from the meridional means for each month. Values start with northern summer and run from May through the seasonal cycle. There is a clear west-to-east movement of the convective maximum which is similar in the three datasets and is traced by a thick dashed line in Fig. 3. It appears near 90°E during the Indian monsoon season in northern summer (June–September), moves eastward to another relative maximum in January and February in the longitudes of Indonesia and Australia

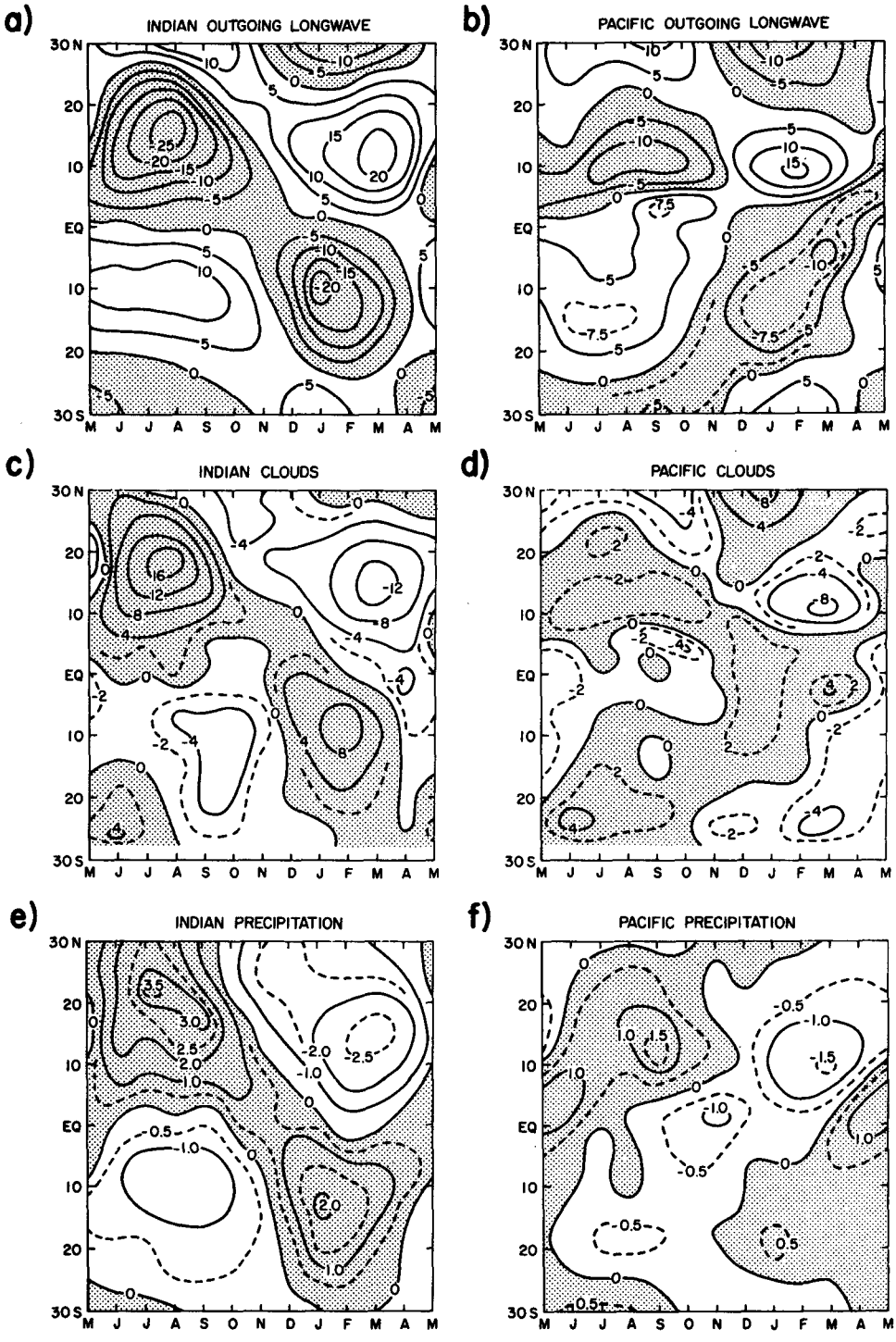


FIG. 2. Annual march of regional zonal means given as monthly deviations from the annual regional zonal means for the Indian (45°–155°E) and Pacific (155°E–95°W) sectors. (a) Outgoing longwave radiation (W $m^{-2}$) for period June 1974–August 1982 (1978 missing), Indian sector; (b) outgoing longwave radiation for Pacific sector; (c) long-term (1966–73) fractional cloudiness (%) for the Indian, and (d) Pacific sectors; (e) long-term precipitation (mm $d^{-1}$) for the Indian, and (f) Pacific sectors. Stippled areas denote greatest cloudiness and precipitation.

during the monsoon season there (roughly 105°–155°E), and then trails eastward over the Pacific in a less well-defined maximum during March and April. A similar calculation was performed with the same data but with the zonal average of the meridional means for each month subtracted from the meridional means at each longitude. A similar pattern to that in Fig. 3 was produced. These results indicate that the west/east asymmetries during the annual cycle are such that strong convection in the western portion of the Indian–Pacific sector is associated with relatively weaker convection in the eastern portion, and vice versa both in terms of the annual cycle at each longitude and at each latitude.

Another interesting feature of Fig. 3 is that even though the convective maximum moves from north to south and back again during the course of the year (Fig. 2), it is stronger as it moves southward and eastward from northern summer to northern winter than on its return journey northward and westward in the Indian sector. This is evidenced by the nearly continuous stippling following the dashed line in Fig. 3 during northern fall. This characteristic was noted by Heddinghaus and Krueger (1981). Their "spring–fall" (second) eigenvector showed the ITCZ had greater strength in northern fall than northern spring. This also can be seen qualitatively in Fig. 1 where stippled areas indicating heavy convection over Southeast Asia are noticeably larger in October (Fig. 1b) compared to April (Fig. 1d). The geography of the Indian–Australian region is such that southern Asia, the island continent of Southeast Asia, and Australia lie in a northwest to

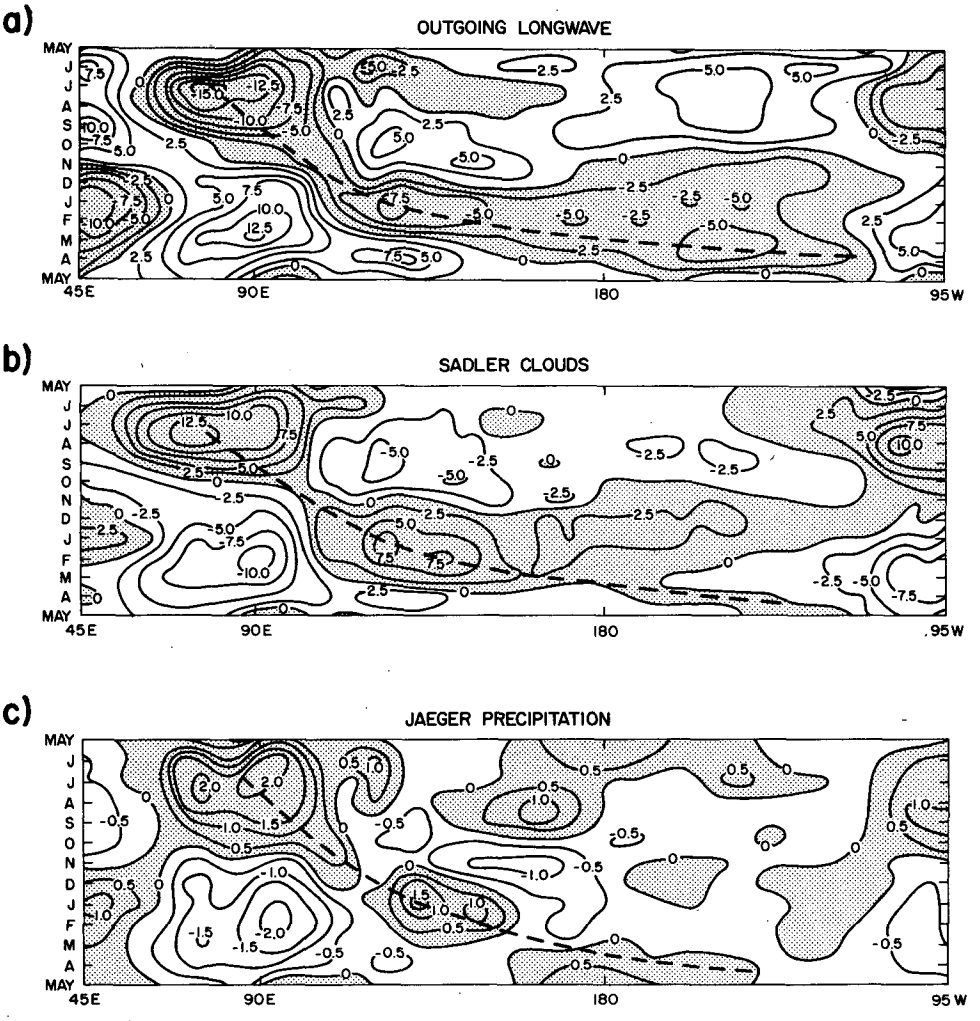


FIG. 3. Annual cycles of meridional means, 30°N–30°S, represented as deviations of monthly meridional means from the annual mean. (a) Outgoing longwave radiation (W $m^{-2}$) for period described in Fig. 2; (b) fractional cloudiness (%) for period described in Fig. 2; (c) precipitation (mm $d^{-1}$). Stippled areas denote greatest cloudiness and precipitation. The thick dashed line follows the course of the strongest area of convection, termed the convective maximum, as it moves from India to the Pacific during the course of the annual cycle.

southeast configuration. It is likely that this induces a diagonal north-to-south and west-to-east movement of the convective maximum from northern summer to winter. As the heavy convection moves further east into the Pacific, convection to the west, over Southeast Asia during the south-to-north and east-to-west movement from northern winter to summer, would be relatively suppressed and therefore would be weaker than during northern fall. The probability that the diagonal arrangement of land masses in this region forces the

TABLE 1. Stations, locations, periods of record (indicating missing full years) and number of strong and weak annual cycles since 1900. Due to some missing months, the number of strong and weak annual cycles is given as a range of fewest to most monthly means available for compositing the annual cycles.

| Station | Location (deg) | Record | Strong | Weak |
|---|---|---|---|---|
| Bombay | 18.9N, 72.8E | 1878–1983 (all) | 27–29 | 28–30 |
| Calcutta | 22.5N, 88.3E | 1878–1983 (all) | 28–29 | 29–30 |
| Port Blair | 11.7N, 92.7E | 1868–1983 (3 yrs missing) | 24–27 | 25–28 |
| Bangkok | 13.7N, 100.5E | 1931–1983 (all) | 16–18 | 16–19 |
| Singapore | 1.4N, 103.9E | 1911–1983 (6 yrs missing) | 19–23 | 21–24 |
| Cocos | 12.2S, 96.8E | 1952–1983 (all) | 10–11 | 6–7 |
| Jakarta | 6.2S, 106.8E | 1864–1983 (6 yrs missing) | 18–19 | 12–13 |
| Dili | 8.6S, 125.6E | 1952–1983 (7 yrs missing) | 7–9 | 4–5 |
| Broome | 18.0S, 122.2E | 1951–1983 (all) | 10–11 | 10–11 |
| Darwin | 12.4S, 130.9E | 1882–1983 (all) | 28–29 | 28–30 |
| Thursday Island | 10.6S, 142.2E | 1951–1983 (all) | 9–11 | 10–11 |
| Port Moresby | 9.4S, 147.2E | 1903–1983 (all) | 25–27 | 26–29 |
| Noumea | 22.3S, 166.5E | 1941–1983 (all) | 13–14 | 13–14 |
| Vila | 17.8S, 168.3E | 1948–1983 (all) | 10–12 | 10–12 |
| Lauthala Bay | 18.2S, 178.5E | 1921–1981 (all) | 20–21 | 20–21 |
| Apia | 13.8S, 171.8W | 1890–1983 (all) | 25–29 | 27–30 |
| Aitutaki | 18.8S, 159.8W | 1931–1981 (all) | 16–18 | 15–17 |
| Rarotonga | 21.2S, 159.8W | 1907–1983 (all) | 24–25 | 25–27 |
| Tahiti | 17.6S, 149.6W | 1935–1983 (all) | 14–17 | 15–17 |
| Rapa | 27.6S, 144.3W | 1952–1983 (all) | 10–11 | 10–11 |
| Pitcairn | 24.1S, 130.1W | 1940–1981 (6 yrs missing) | 11–12 | 11–12 |
| Ocean Island | 0.9S, 169.5E | 1921–1981 (5 yrs missing) | 15–19 | 16–19 |
| Tarawa | 1.4N, 172.9E | 1951–1983 (all) | 10–11 | 9–11 |
| Funafuti | 8.5S, 179.2E | 1932–1983 (all) | 15–18 | 15–18 |
| Canton | 2.8S, 171.7W | 1937–1967 (1 yr missing) | 7–8 | 8–9 |
| Puka Puka | 10.9S, 165.8W | 1932–1981 (2 yrs missing) | 11–14 | 11–14 |
| Penrhyn | 9.0S, 158.1W | 1937–1981 (all) | 13–15 | 12–14 |
| Fanning | 3.9N, 159.4W | 1922–1970 (30 yrs missing) | 3–4 | 3–5 |

convection to follow a similar path due to differential heating of land and sea is given support by GCM results presently being prepared for publication.

To further examine the annual cycle of the convective maximum, 28 stations were selected stretching from India east to the Pacific. Selections were made based on homogeneity and record length as well as position relative to the areas of maximum convection in Fig. 1. The stations are listed in Table 1 along with their location and length of record. The dots in Fig. 1 refer to the location of the stations in Table 1. The stations also are labeled on the geographic maps (Figs. 7 and 8).

Figure 4 shows the long-term mean annual cycle, May to April, of sea level pressure and precipitation for each of the stations as deviations of three-month running means from the anual mean. The stations in this figure are arranged to follow the convective maximum from India southeastward to the SPCZ; stations northeast of the SPCZ region are furthest to the right. In Fig. 4a lowest pressure generally occurs during the time of year with greatest precipitation in Fig. 4b. The transition of the seasonal minimum of sea level pressure is fairly rapid from northern to southern hemisphere, but the associated rainfall maximum more smoothly traverses from north to south and west to east as was seen in Figs. 2 and 3 for the OLR and precipitation. The stations in the western equatorial Pacific, from Ocean Island to Penrhyn in Fig. 4c, experience a northern winter rainfall maximum which also can be inferred from Fig. 1. Fanning Island, the easternmost station which lies near the ITCZ north of the equator, experiences a seasonal rainfall maximum during March–June. This eastward movement of the long-term mean rainfall maxima into the ITCZ at this time of year was noted in Figs. 1 and 3.

## 4. Interannual variability

Results presented in the previous section agree with other observational studies (e.g., Lau and Chan, 1983b; Heddinghaus and Krueger, 1981) in that the long-term mean annual cycle of the convective maximum is strongest during its southeastward traverse from northern summer in the Indian monsoon to northern winter in the Australian monsoon and SPCZ. It was also noted in Fig. 3 that east–west linkages appeared such that strong convection in the Indian sector is associated with weaker convection over most areas of the Pacific sector, and vice versa, during the course of the mean annual cycle. Such east–west connections were noted earlier to be linked with variability in those years associated with the SO, in particular, with regard to Asian monsoon and Pacific rainfall. To further inves-

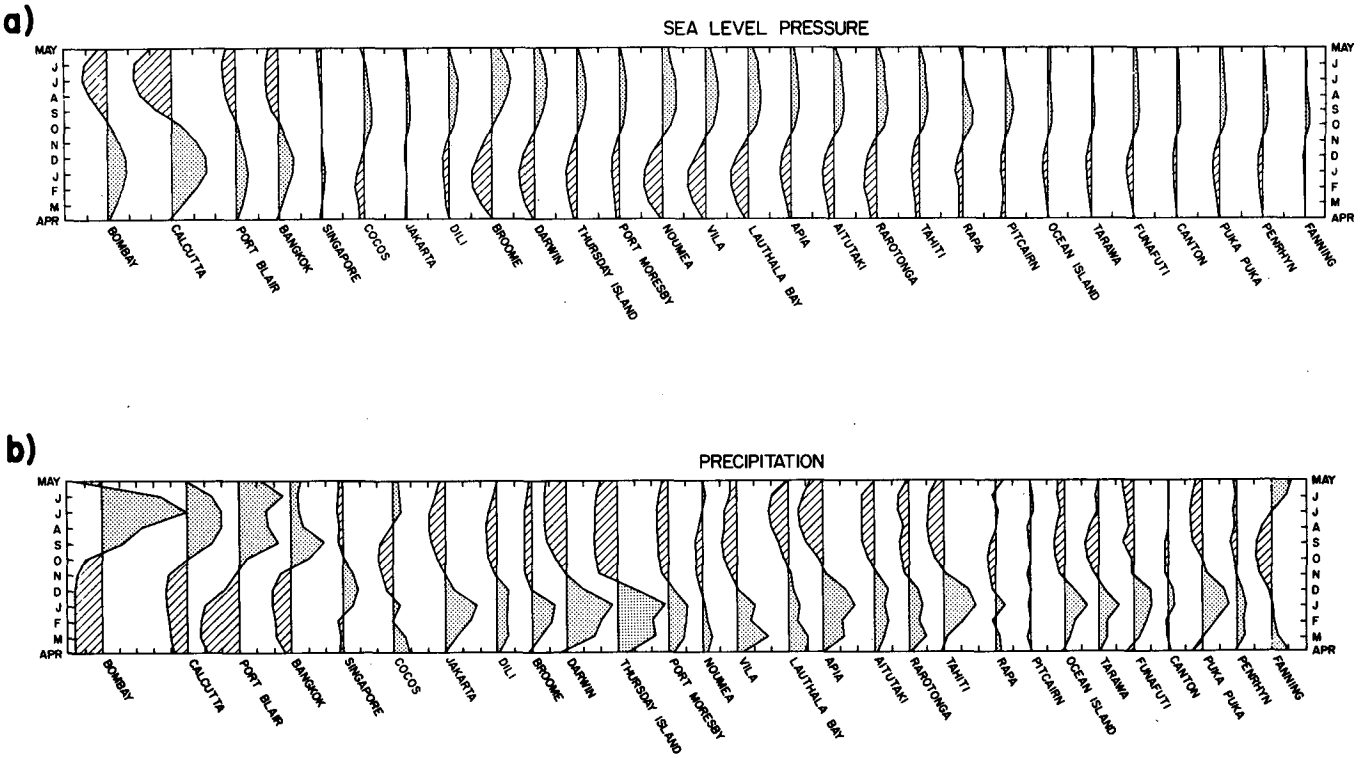


FIG. 4. Annual cycle of long-term mean station data (stations are listed in Table 1) for (a) sea level pressure (SLP), (b) precipitation, plotted as deviations of three month running means from annual mean. Stippling denotes highest SLP (a), and greatest precipitation (b); vice versa for cross-hatching. Each tic mark on horizontal axes indicates (a) 5.0 mb, (b) 100 mm/mo.

tigate the interannual variability of the east–west linkages between the Indian and Pacific sectors, it would be desirable to choose a long-term index of precipitation or convective activity as a starting point. Since convection and rainfall associated with the Indian monsoon during northern summer begins the southeastward surge of the convective maximum from northern summer to northern winter in the mean seasonal cycle, an index of Indian monsoon rainfall would appear to be a convenient indicator to identify relatively stronger or weaker convective activity in that region. Obviously interannual variation is hard to categorize as a series of discrete events. To pick a "starting point" in the continually evolving set of processes is clearly somewhat arbitrary. However the extreme seasons provide a logical place to begin to look for associations, and northern summer and the Indian monsoon is a good place to begin for reasons already mentioned in terms of the mean annual cycle. In addition, Gordon (1986) has computed lagged autocorrelations for the Southern Oscillation Index (SOI) which show that May–July are strongly correlated with succeeding months through the following April, but are only weakly correlated with preceding months. He is one of the more recent investigators to suggest that the SOI is best described by an annual cycle which runs from May through the following April. Earlier studies by Troup (1965) and others first demonstrated this relationship.

A long-term record of Indian monsoon rainfall has been compiled by Verma et al. (1984) and reproduced in Fig. 5. The period of record is from 1881 to 1983 and is an update of the series published by Parthasarathy and Mooley (1978). "Strong" and "weak" years are defined from Fig. 5 as relative minima or relative maxima in monsoon precipitation. That is, a "strong" year is one in which the monsoon rainfall is greater than both the year before and the year after, and vice versa for "weak" years. Very few of the station records to be subsequently analyzed extend back to before 1899. Therefore, strong and weak years were identified for the period 1899–1983. This provided 83 possible years for analysis since the first and last years could not be considered by definition. The relatively strong and weak years are listed in Table 2. Due to the tendency of Indian monsoon rainfall to have a significant biennial component (Bhalme and Jadhav, 1984) these two sets of years are not totally independent. Other measures associated with interannual variability in the Indian and Pacific sectors also show a notable biennial component (e.g., Nicholls, 1979). Spectra for SSTs in the eastern tropical Pacific and the Tahiti minus Darwin normalized surface pressure difference both show peaks near 24 months (Rasmusson and Carpenter, 1982).

Since "strong" and "weak" annual cycles are strong or weak relative only to the preceding and following years, these two sets of years should be expected to produce opposite conditions. For example, out of 29 relatively strong monsoons in Table 2, 17 are preceded by a relatively weak monsoon. For 30 relatively weak monsoons, 23 are preceded by a relatively strong monsoon. There are 24 years in this compilation since 1900 that are neither relatively strong or relatively weak. Extreme events in the SO, Warm and Cold Events, are also reflected in the list of relatively strong and weak monsoons. There have been 16 Cold Events since 1900 listed by van Loon and Shea (1985), and ten of these are associated with relatively strong monsoons. Of the 19 Warm Events since 1900 listed by van Loon (1984), 14 occurred in conjunction with relatively weak monsoons. Only one Warm Event took place during a relatively strong monsoon, and only two Cold Events occurred during a relatively weak monsoon.

Using the relatively strong and weak monsoon years listed in Table 2 as a starting point, differences are computed from the preceding years for the annual cycle from the beginning of the Indian monsoon season in May to the following April. Since there is the aforementioned biennial tendency, the strong and weak

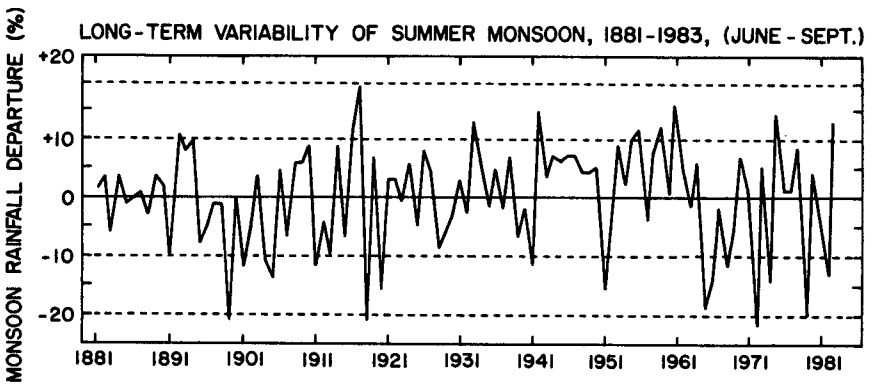


FIG. 5. Indian monsoon rainfall, 1881–1983, expressed as a percentage departure from the long-term mean. Values averaged over India for June–September are adapted and updated by Verma et al. (1984) from series published by Parthasarathy and Mooley (1978).

TABLE 2. Relatively strong or weak Indian monsoons based on Fig. 6. "Strong" refers to relatively greater rainfall during monsoon season than the year before or the year after, vice versa for "weak." Years with asterisks are present in the Southern Hemisphere gridded sea level pressure dataset used for composites in Fig. 14. CE and WE refer to Cold and Warm Events defined by van Loon and Shea (1985) and van Loon (1984), respectively.

| Strong | | Weak | |
|---|---|---|---|
| 1900 | 1942(CE) | 1901 | 1941 |
| 1903(CE) | 1944 | 1905 | 1943 |
| 1906(CE) | 1950 | 1907 | 1945 |
| 1910 | 1953(WE)* | 1911(WE) | 1951(WE)* |
| 1912 | 1956* | 1913(WE) | 1954(CE)* |
| 1914 | 1959 | 1915 | 1957(WE)* |
| 1917 | 1961 | 1918(WE) | 1960 |
| 1919 | 1964(CE) | 1920(CE) | 1963(WE) |
| 1924(CE) | 1967 | 1923(WE) | 1965(WE) |
| 1926 | 1970(CE) | 1925(WE) | 1968 |
| 1931(CE) | 1973(CE)* | 1928 | 1972(WE)* |
| 1933 | 1975* | 1932(WE) | 1974* |
| 1936 | 1978(CE)* | 1935 | 1976(WE)* |
| 1938(CE) | 1980* | 1937 | 1979* |
| 1940 | | 1939(WE) | 1982(WE)* |

* Years present in SH gridded sea level pressure data.

composite differences are almost mirror images of each other with the signs reversed. Therefore in the analyses to follow, results will be shown only for the composites based on the relatively strong monsoon years. These will be referred to as the strong annual cycles or simply the strong years, again taken as an annual cycle running from May through the following April. Results for the weak years are not shown but can be inferred as the near mirror images, with signs reversed, of the strong years.

Since there is some doubt as to the usefulness of looking only at pair-year differences, differences are also computed for the strong and weak years from the long-term annual means. Again these results will be shown only for the strong composites. The weak composites are very nearly the opposite pattern, with signs reversed, of the strong composites.

Differences of three-month running means for the set of strong years listed in Table 2 minus the previous years are shown for sea level pressure (SLP) and precipitation in Fig. 6. Significance at the 5% and 1% levels is indicated for sea level pressure. Given the many difficulties in analyzing precipitation data, the precipitation difference values are shown only to give a qualitative feeling for the relative changes of rainfall associated with the changes of SLP.

Figure 6 shows that a strong year, which begins during a relatively more active Indian monsoon, is associated with lower sea level pressure and greater precipitation during the monsoon season June–September at Bombay, Calcutta, and Port Blair. Calcutta only shows greater precipitation and lower SLP late in the monsoon season. Bombay is the more consistent indicator of relatively stronger monsoon activity in the monsoon index averaged over all of India with lower SLP and higher rainfall throughout the monsoon season. However, at the same time stations to the southwest are experiencing significantly altered conditions. Stations in the region of the Australian monsoon—Jakarta, Dili, Broome, Darwin, Thursday Island, and Port Moresby—have significantly lower SLP and higher temperatures at this time of year. Even stations as far to the southeast as Noumea and Vila near the SPCZ in the Pacific show similar characteristics.

As the convective maximum moves southeast the Australian monsoon is more intense during northern winter as evidenced by very low SLP and associated large increases in seasonal rainfall. Stations in the SPCZ experience similar conditions. Stations to the east of the SPCZ in the tropical Pacific undergo opposite conditions as they are under the influence of relatively higher pressure in the South Pacific High.

To summarize the information in Fig. 6, geographical plots are shown for four representative months in Figs. 7 and 8. These show the areas of similar signs for the differences plotted in Fig. 6. It can be seen that, for example, during the first part of a strong annual cycle (July, October) the sea level pressure is lower to the west and south and higher to the north and east of a line stretching very near the long-term mean position of the SPCZ in Fig. 1. This is associated with lower SLP in those regions particularly in July and October over northern Australia and in the southwest part of the SPCZ area. Anomalous cyclonic flow associated with lower pressure to the west and anomalous anticyclonic flow associated with the higher pressure to the east of the SPCZ results in anomalous westerly flow north of Australia, and southeastward flow from the deep tropics and increased convergence in the SPCZ. This is evidenced by greater precipitation along the axis of the SPCZ and to the southwest. This also could be interpreted as a shift to the southwest of the active region of the SPCZ. For example, even though Apia is in a region of higher pressure to the east of the SPCZ axis in Fig. 7, it experiences greater precipitation because of increased convergence in the SPCZ itself. Meanwhile, stations farther north and east in the tropical Pacific undergo decreases of precipitation to go along with increased intensity of the South Pacific High. January is characterized by the shift of seasonal rainfall into the Pacific as the convective maximum moves into the SPCZ. Finally, in April relatively lower SLP has extended east to Pitcairn and has begun to erode the strength of the South Pacific High.

Since many of these effects have been noted in other studies to occur in association with the extremes of the SO, namely Warm and Cold Events, and since it was pointed out in Table 2 that Cold and Warm Events usually correspond to relatively strong and weak monsoons respectively, it could be possible that the results in Fig. 6 are merely a reflection of the dominant SO signal in those sets of years. Therefore similar pair-year

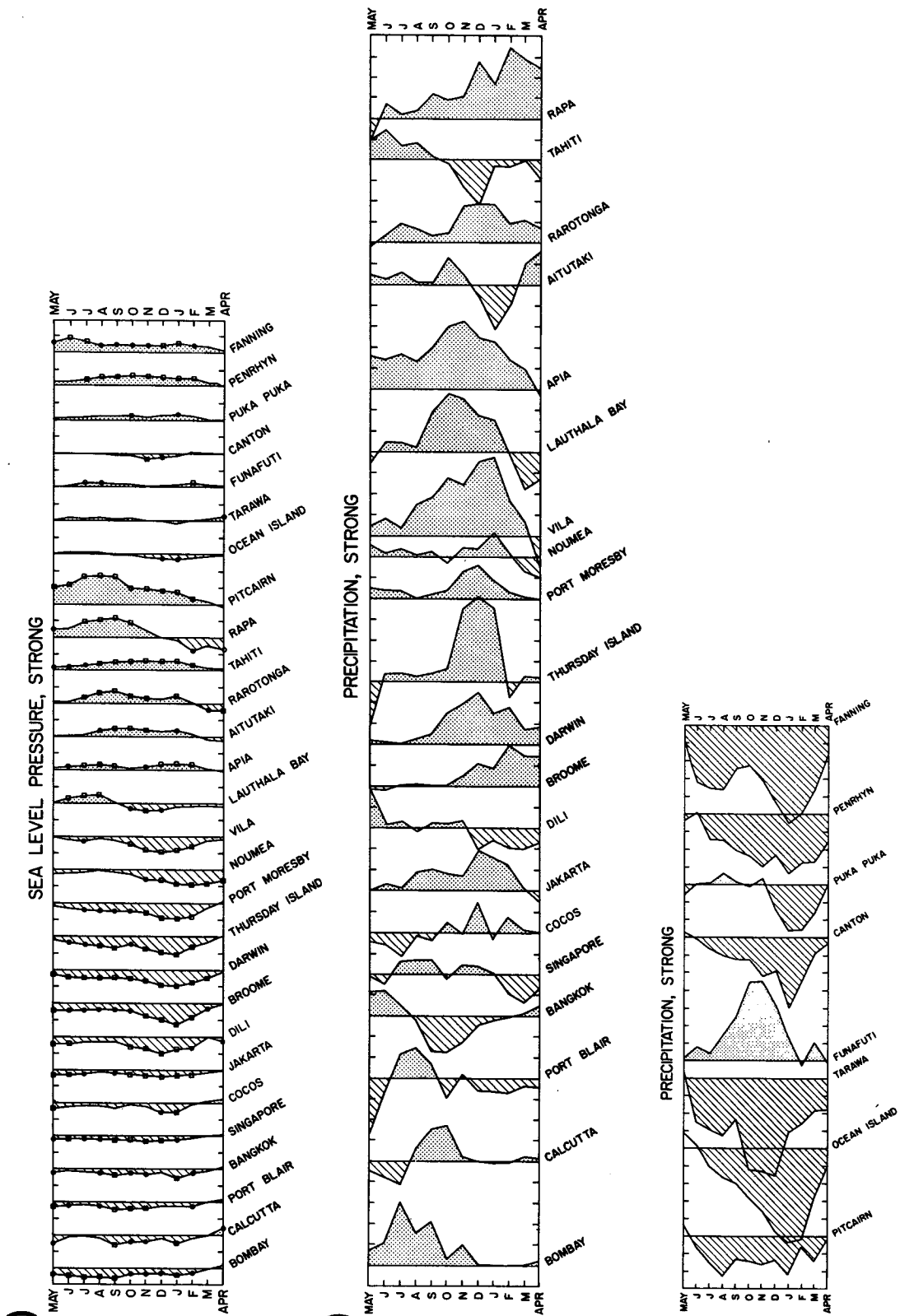


FIG. 6. Based on relatively strong monsoon years in Fig. 5 listed in Table 2 (see text), differences of three-month running means of relatively strong annual cycles minus the previous years' annual cycles are shown for stations listed in Table 1 for (a) SLP, and (b) precipitation. Stippling denotes higher SLP (a), and greater precipitation (b) during strong annual cycles; vice versa for cross-hatching. Significance is shown at the 5% level (circles) and 1% level (squares). Each tic mark on horizontal axes indicates (a) 1.0 mb, and (b) 20.0 mm/mo.

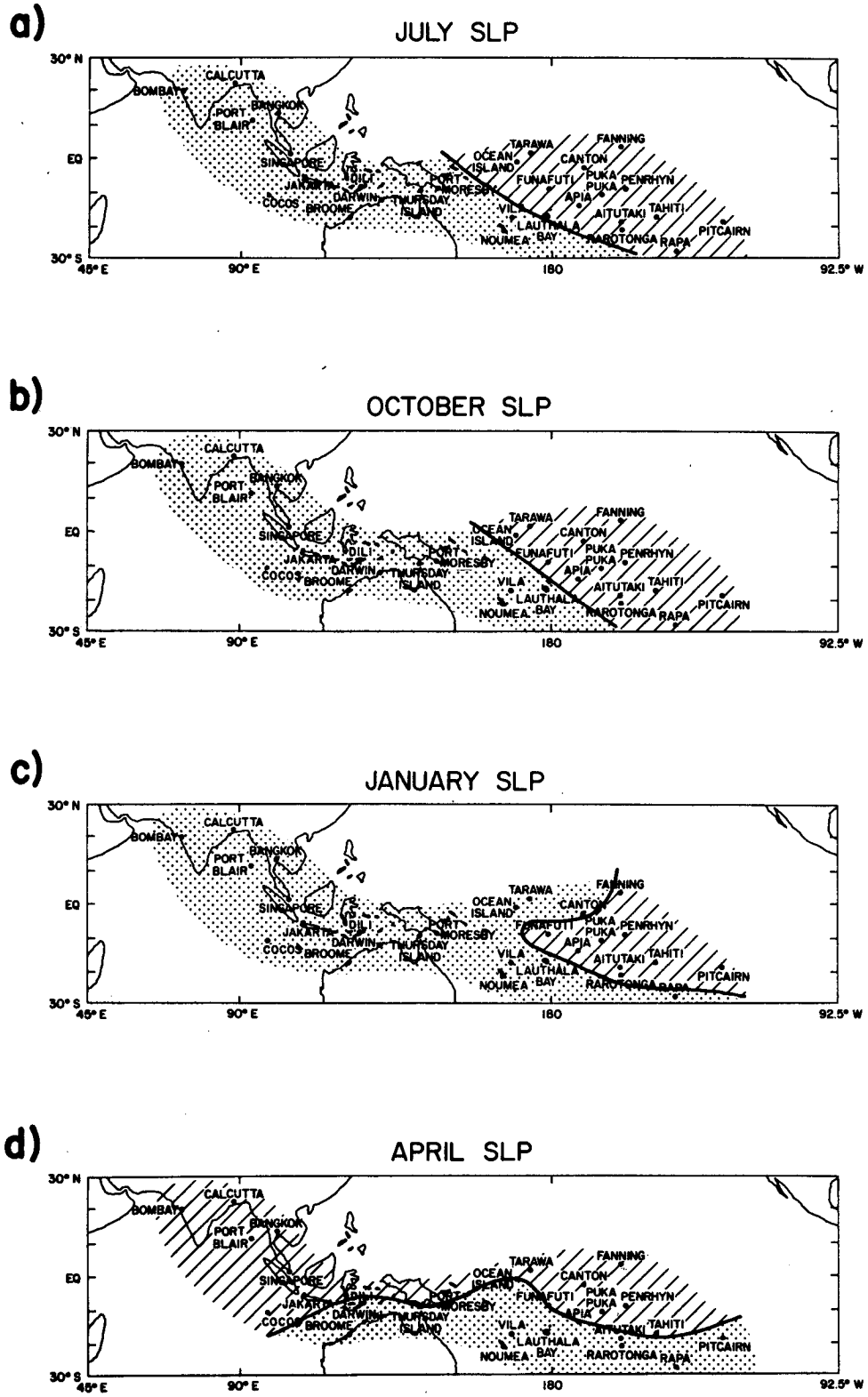


FIG. 7. Geographical plot of stations listed in Table 1. Areas of same sign are shown for strong annual cycle minus previous annual cycles for SLP during four representative months—(a) July, (b) October, (c) January and (d) April. Actual values for all months are shown in Fig. 6. Stippling denotes lower SLP and cross-hatching higher SLP during a relatively strong annual cycle. Pattern is very nearly opposite for weak annual cycles.

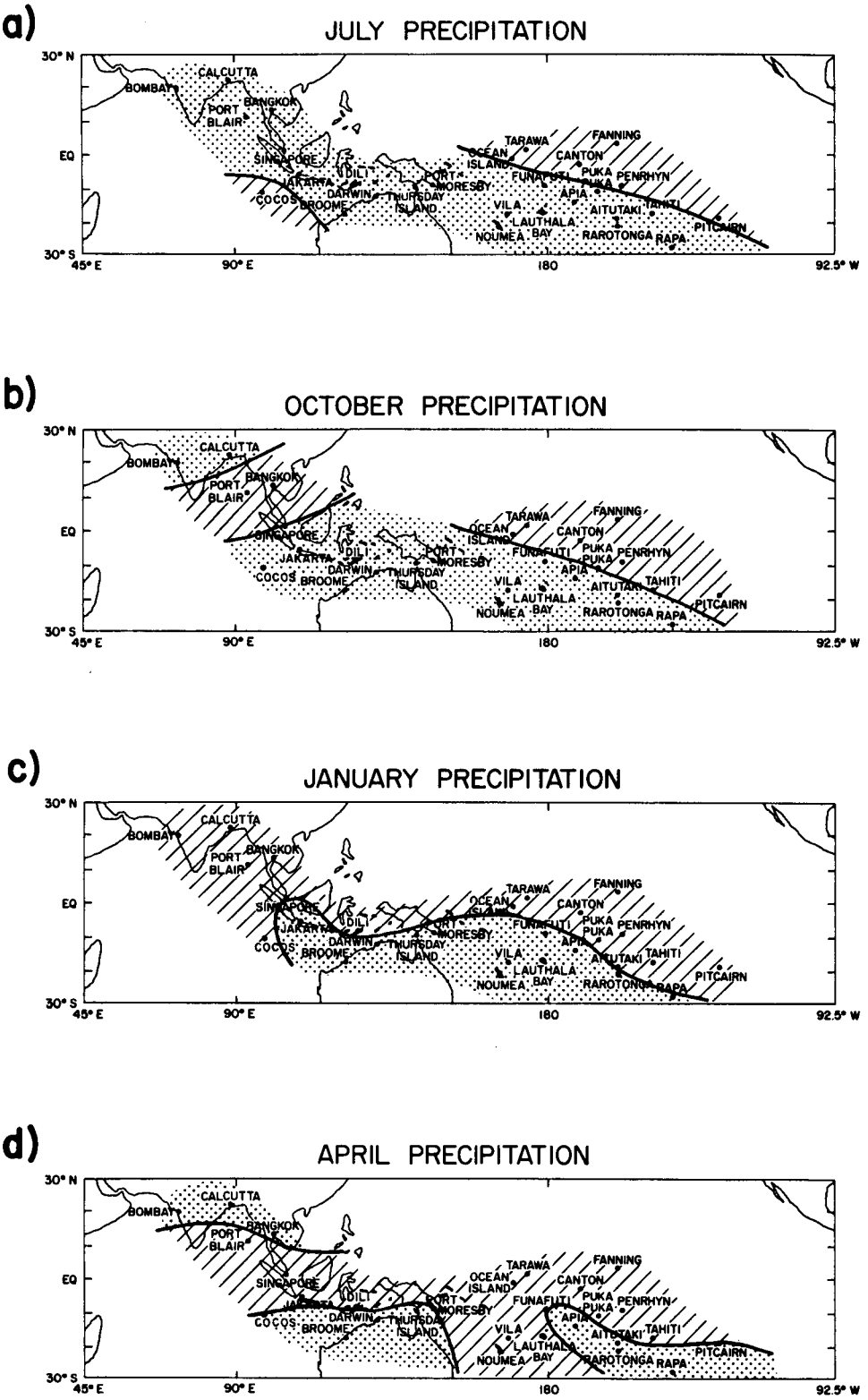


FIG. 8. As in Fig. 7 except for precipitation. Stippling denotes higher precipitation during a relatively strong annual cycle, vice versa for cross-hatching. Patterns are nearly opposite for weak annual cycles.

differences of SLP are computed for strong years which are Cold Events (CE) (Fig. 9a) and for strong years which are not CEs (Fig. 9b). It can be seen that the signal in Fig. 6 is stronger and more dominant for the CE years in Fig. 9a. However, the same signal, albeit with reduced magnitude, is present in the strong years without CEs. Results for precipitation differences (not shown) show similar signals. Therefore, it appears that the extreme events of the SO, CEs, display the largest signal but other seasonal cycles which begin in northern summer with a relatively strong monsoon show a similar signal but with reduced magnitude. For many stations this involves lower SLP and increased rainfall to the west of the SPCZ axis, higher SLP and decreased rainfall to the east of the SPCZ axis throughout most of an annual cycle, May through the following April, in CE years. In strong years without CEs, this effect is not as pronounced throughout the year, but is seen more as a local enhancement of seasonally lower pressure and higher rainfall either immediately preceding or during the local rainy season. This is particularly evident for Bombay in northern summer, and for the Australian monsoon-area stations of Jakarta, Dili, Broome, Darwin, Thursday Island and Port Moresby.

Since interpretation of pair-year differences may not be as meaningful as differences computed from the long-term mean, the latter such calculations also were performed for SLP and precipitation. For consistency the annual cycle of long-term monthly means is taken as three-month running means computed for each station. Results for SLP are shown in Fig. 10 with significance at the 5% and 1% levels as before for the strong years listed in Table 2. It can be seen that the results are similar to those shown in Fig. 6 for the pair-year differences with somewhat reduced magnitudes. This is not surprising considering that the strong and weak years listed in Table 2 make up over two thirds of all years since 1900 and oscillate about and define the long-term mean. In other words, the difference of a strong year from the preceding year, which was seen to most likely be a weak year, is larger but of the same sign as that year subtracted from the long-term mean.

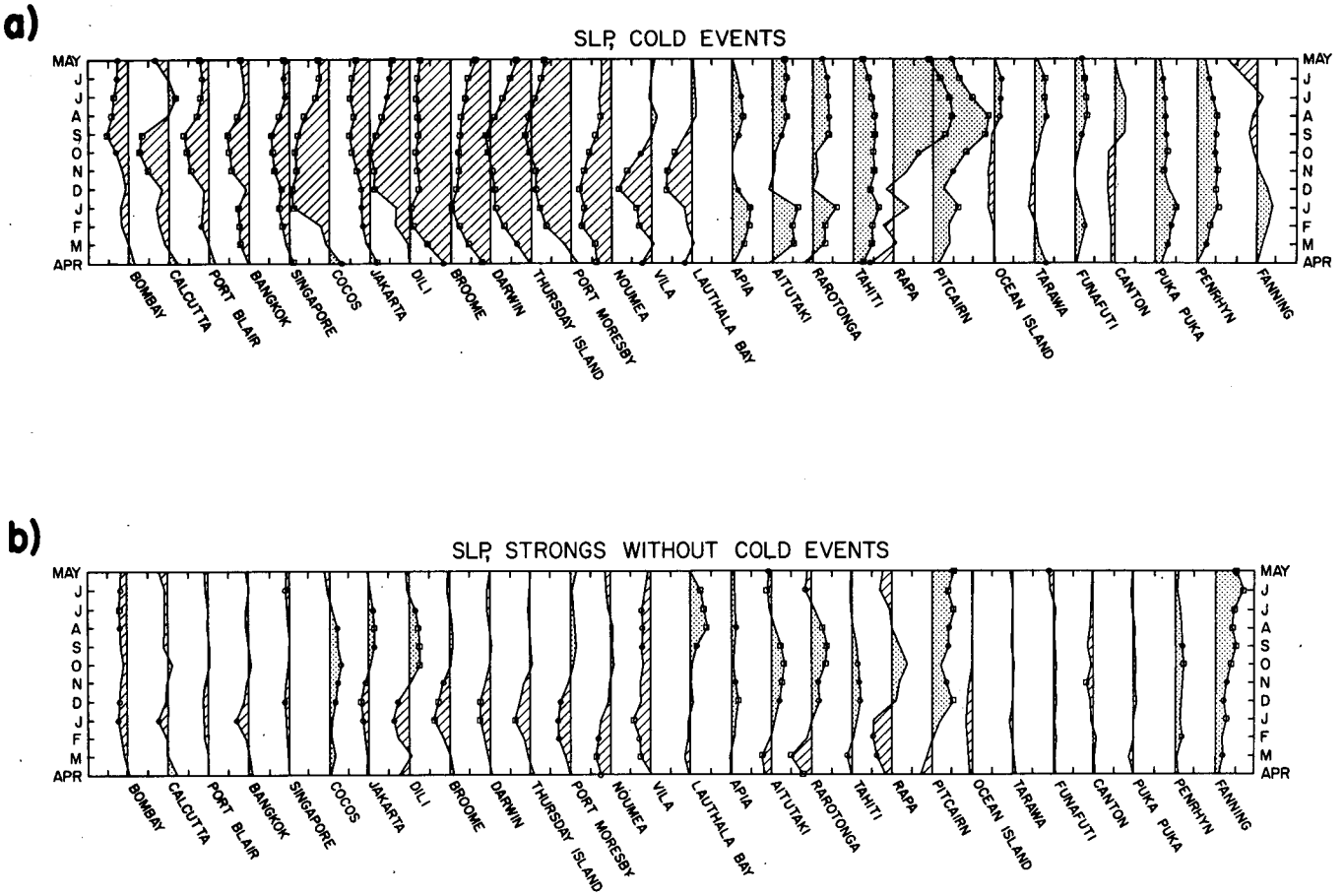


FIG. 9. Differences of three-month running means minus the previous year for sea level pressure in (a) relatively strong years which are also Cold Events noted in Table 2, and (b) relatively strong years which are not Cold Events in Table 2. Stippling denotes higher SLP during strong years, relatively lower SLP is cross-hatched. Significance is shown at the 5% level (circles) and the 1% level (squares). Each tic mark on the horizontal axes indicates 1.0 mb.

This is in spite of the fact that the strong and weak monsoon years were defined only in relation to the preceding and following years' monsoon rainfall amount, not in relation to long-term mean monsoon rainfall. This indicates that monsoon rainfall over India is probably only an indicator of relative precipitation over the much larger summer monsoon area, encompassing most of southern Asia and the northern Indian Ocean.

Differences of SLP for strong years with CEs only and other strong years which are not CEs minus the long-term monthly means are also computed. Results are similar to those shown in Fig. 9. The CE strong years (not shown) had the larger and more significant signal, but the annual cycle of the differences for the stations was similar to the differences shown in Figs. 6 and 9. The differences for the strong years without CEs from the long-term mean in Fig. 10b show that the signal is very small in the Indian summer monsoon region. Bombay is again the best indicator with lower pressure during northern summer. Stations east of the SPCZ, such as Lauthala Bay, Apia, Aitutaki, Pitcairn, Funafuti, and Fanning show a larger signal of higher pressure during northern summer. The Australian monsoon-area stations mentioned earlier again show a local enhancement of lower pressure and precipitation either just before or during their respective rainy seasons.

## 5. Sea surface temperature

Due to the importance of dynamically coupled interactions between atmosphere and ocean, differences for the strong and weak composites in Table 2 are computed for SSTs from COADS. As noted by van Loon and Shea (1985), the major contribution to the areal coverage of the COADS data comes after 1950. Therefore, strong and weak pair-year differences are computed for the post-1950 period using three-month running means. Results for the strong years minus the preceding years are shown in Fig. 11 for four representative months: July, October, January and April. Stippled areas indicate warmer SSTs during a strong annual

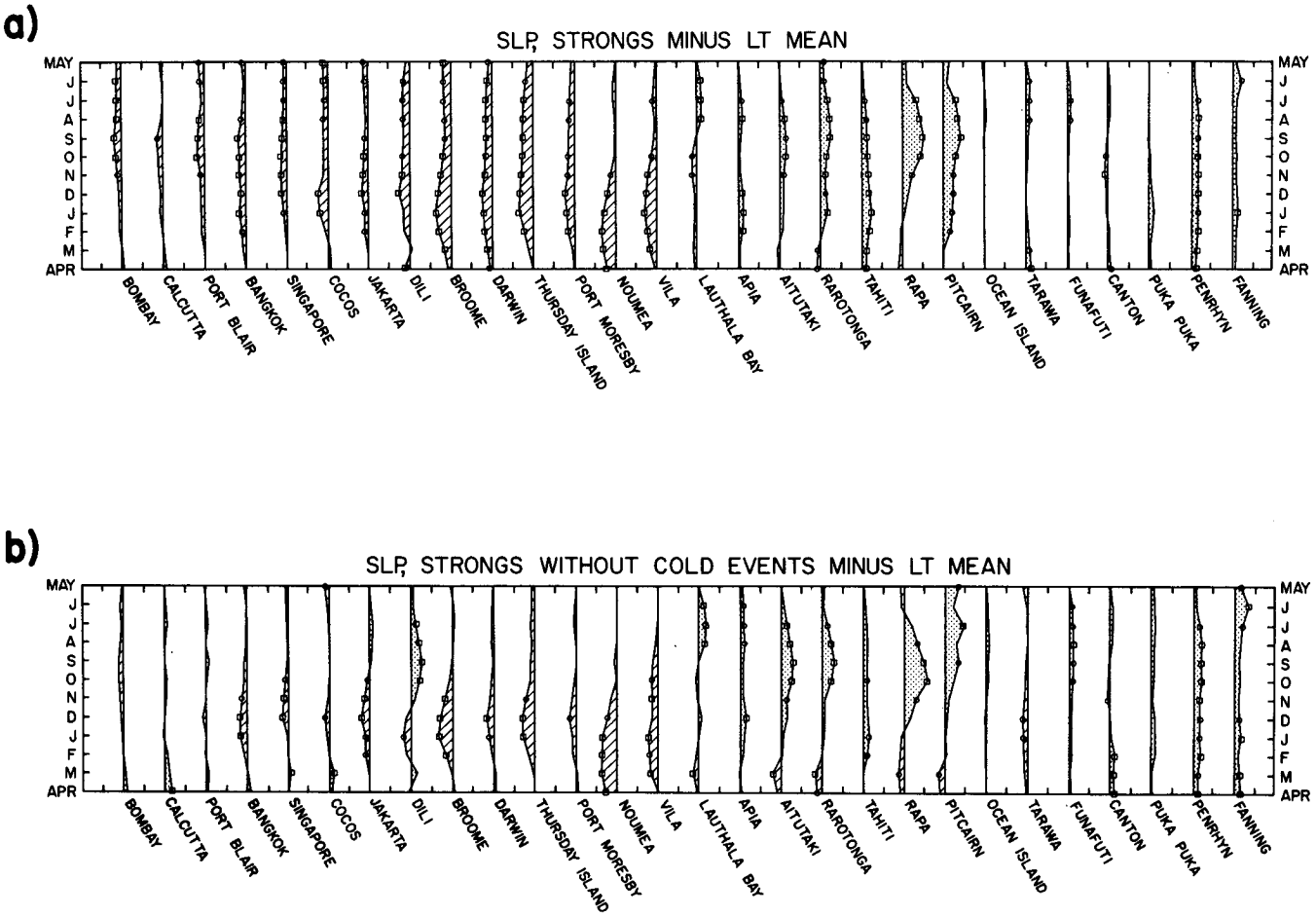


FIG. 10. As in Fig. 9 except monthly mean SLP differences are computed from long-term mean annual cycle of monthly means for (a) all strong years listed in Table 2 and (b) strong years which are not denoted as Cold Events in Table 2.

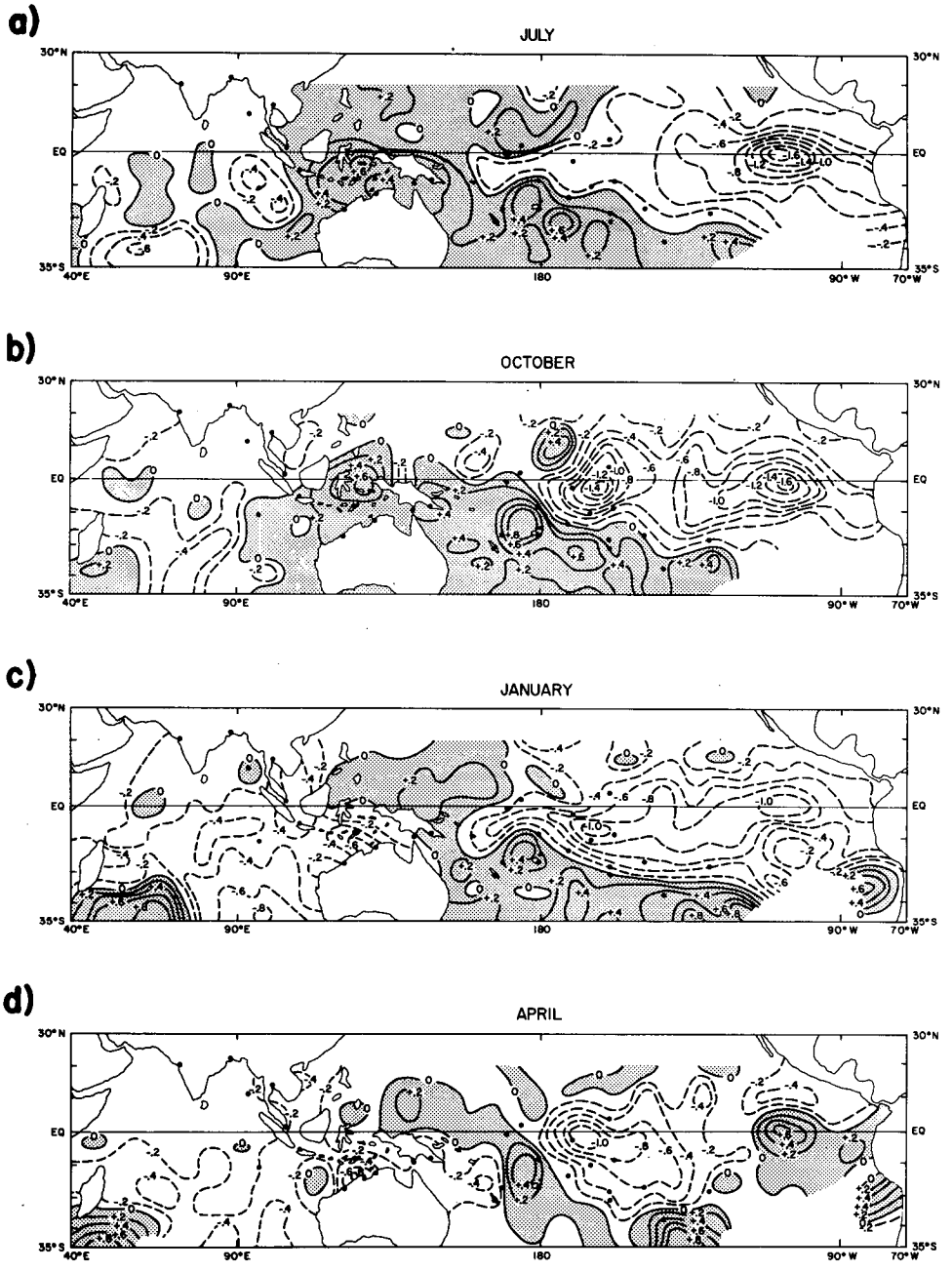


FIG. 11. Sea surface temperature differences for all strong years listed in Table 2 minus the previous years for (a) July, (b) October, (c) January and (d) April. Positive areas denoting higher SSTs during the strong years are stippled.

cycle. In July (Fig. 11a) and October (Fig. 11b) higher SSTs cover much of Southeast Asia, the area north of Australia, and the SPCZ in the South Pacific, while lower SSTs dominate the eastern tropical Pacific. These areas to the west of the SPCZ correspond to regions with greater precipitation amounts noted in Fig. 8a, b, and vice versa for the areas east of the SPCZ. In January, the relatively stronger Australian monsoon is associated with lower SSTs north of Australia, while higher SSTs persist over the SPCZ region and low SSTS continue in the tropical eastern Pacific. By April, a transition has begun with the area of low SSTs in the tropical Pacific shrinking as high SSTs begin to appear in the equatorial eastern Pacific. In the Indian Ocean, small positive SSTs are present in May (not shown), but by July in Fig. 11a mostly negative anomalies are present which persist throughout the rest of the annual cycle.

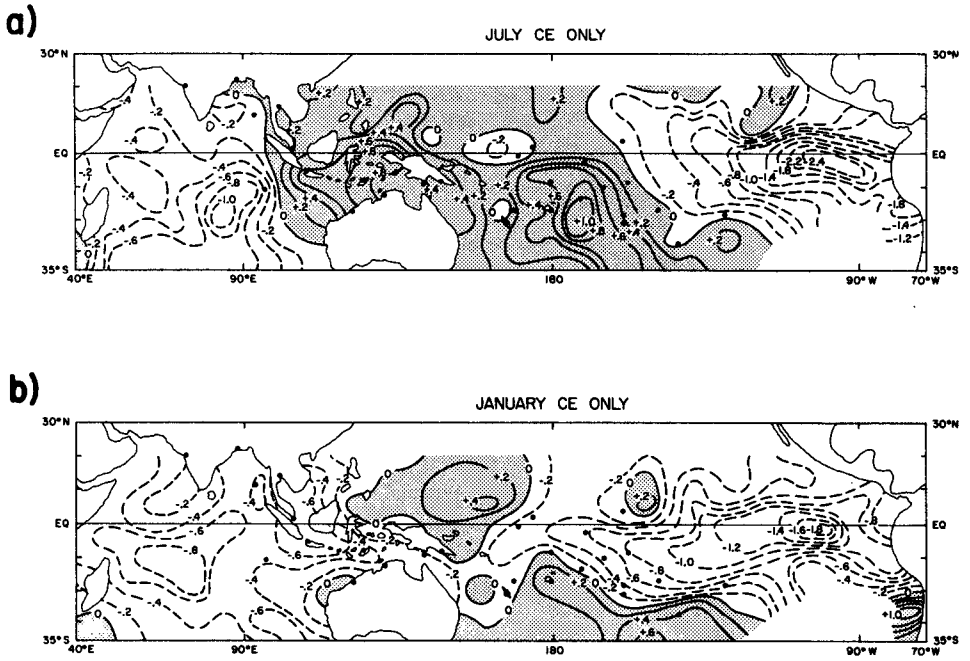


FIG. 12. As in Fig. 11 except only for strong years denoted as Cold Events in Table 2 for (a) July and (b) January.

To investigate the contribution to the strong years from CE years and other years without CEs, pair-year differences for SSTs are computed like those for SLP and precipitation shown earlier. Results for all months in these sets of years are similar to those for corresponding months in Fig. 11. July and January are shown for only Cold Events in strong years (Fig. 12) and for strong years without Cold Events (Fig. 13). Similar to the SLP results, the CE composites show the larger signal, the non-CE years a smaller signal, but

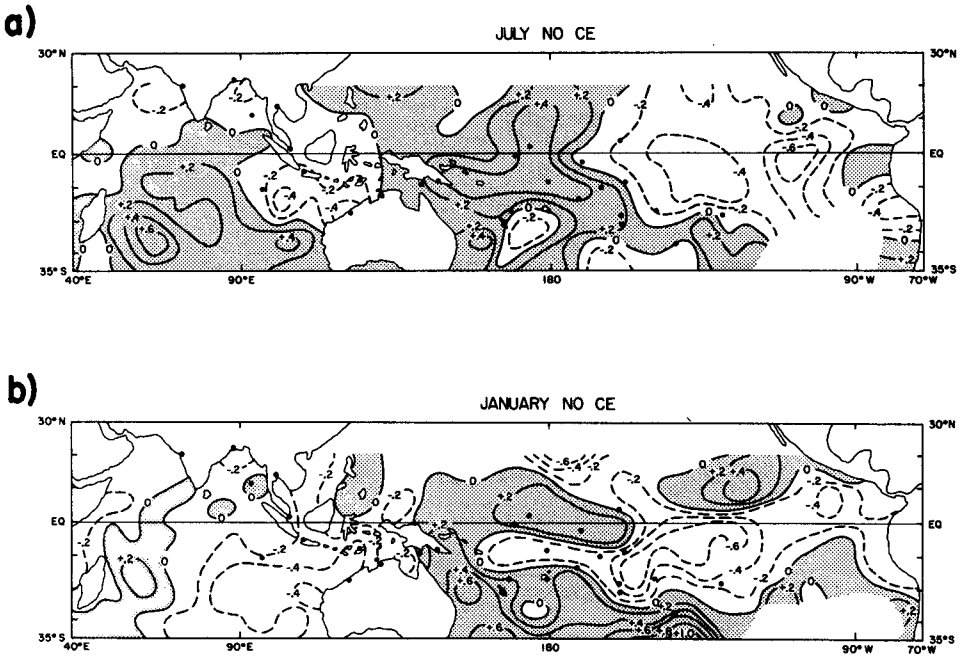


FIG. 13. As in Fig. 11 except only for strong years not denoted as Cold Events in Table 2 for (a) July and (b) January.

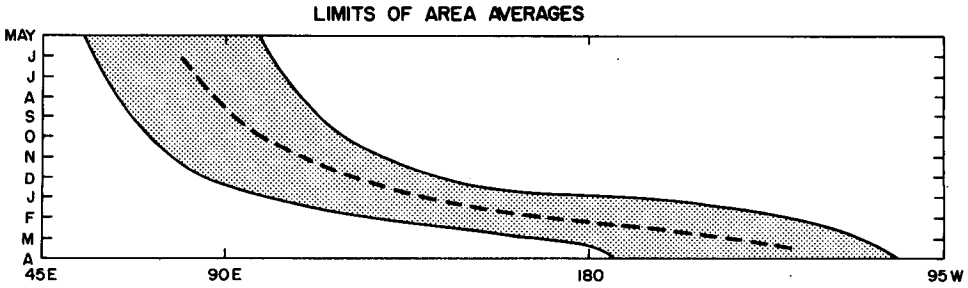


FIG. 14. Longitudinal limits based on the convective maxima in Fig. 3, used to compute area averages 30°N–30°S for individual months.

all years are consistent in the pattern of the differences outlined in Fig. 11. In spite of the noisy nature of the data and the difficulty in performing conventional significance tests with the SSTs, these results are consistent with those from the station SLP analyses. It would appear that the SO extreme years, the CEs, indeed display the dominant anomaly pattern evolution throughout the annual cycle. However, there are other years when the same composite patterns evolve but with much reduced amplitude.

## 6. Outgoing longwave radiation

To examine the year-to-year variations of the convective maximum as it moves from India eastward to the Pacific, a set of area averages are devised to follow the path of the maximum in Fig. 3a for OLR. This is done by taking W–E sectors (the stippled area in Fig. 14) and averaging the individual monthly area averages over the particular W–E spans for each month from 30°N to 30°S.

Due to the break in the OLR data (most of 1978 is missing), the annual cycles of 1977–78 compared to 1976–77, 1978–79 compared to 1977–78, and 1979–80 compared to 1978–79 cannot be considered. Since this particular OLR dataset ends in August 1982, the annual cycle of 1982–83 also cannot be compared to 1981–82. Of the remaining years, 1975 and 1980 are listed as the beginning of relatively strong annual cycles in Table 2, and 1976 and 1981 are listed as the beginning of weak annual cycles.

To portray the mean annual cycle of the convective maximum for the difference between the relatively strong and weak annual cycles, first the preceding annual cycle is subtracted from each strong or weak annual cycle. Then the weak pair year differences are subtracted from the strong pair year differences after which a three-month running mean is computed for the annual cycle of the differences at each longitude. The result is shown in Fig. 15. As expected, heavier convection (larger negative differences) during the strong annual cycles compared to the weak ones lies along the path of the convective maximum denoted by the thick dashed line. Note also the opposition in the sense of the east–west circulation between the Indian and Pacific sectors noted earlier such that stronger convective activity in the western portion is associated with relatively weaker activity in the east, and vice versa. This implies that during a strong annual cycle, there is relatively less convective activity in the eastern Pacific associated with the higher SLP seen for stations in that region.

It is interesting to note that the relatively greater increases in precipitation during strong years for several of the Australian monsoon-area stations (e.g., Cocos, Jakarta, Dili, Darwin, Thursday Island, and Port Moresby in Fig. 6b) occur in November–December just prior to or at the beginning of the local rainy season. This characteristic is reflected in the OLR results in Fig. 15. The largest negative OLR anomaly near 100°–135°E in the area of these stations, indicating greater convection during strong years, also occurs during November–December. Similar effects have been noted by Rasmusson and Carpenter (1982) for Indonesian sta-

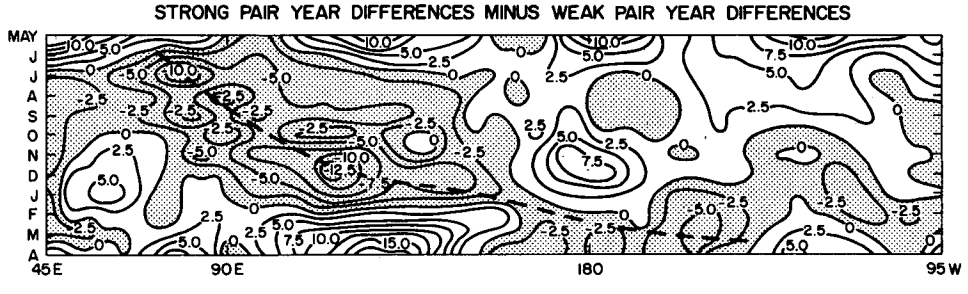


FIG. 15. Available strong pair year difference composites minus weak pair year difference composites for outgoing longwave (W $m^{-2}$). Stippled areas indicate greater convection in the strong annual cycles. The thick dashed line follows the path of the convective maximum similar to that in Fig. 3.

tion rainfall. Their set of years is somewhat different, but average rainfall departure is positive through December of a year prior to a Warm Event in their compilation (comparable here to a strong year).

### 7. Relations to Southern Hemisphere midlatitudes

In section 1 it was noted that the midlatitude circulation in the Southern Hemisphere has a dominant semiannual oscillation such that the circumpolar trough expands and weakens twice a year in June and December (van Loon, 1967). These months are also critical for the onset of the Indian and Australian monsoons. Studies cited previously in section 1 agree that active Asian monsoons are usually associated with strong subtropical highs. Anomalous convection in the tropical Pacific also has been shown to relate to events at higher latitudes taking place in southern fall (e.g., van Loon, 1984; Harrison, 1984; van Loon and Shea, 1985). Therefore, a three-month average is computed for May, June, July (MJJ) when, in the long-term mean, the circumpolar trough is furthest equatorward during the critical transition period for either a strong monsoon or strong convection in the tropical Pacific.

Figure 16 shows composite differences for relatively strong annual cycles (Fig. 16a) and weak annual cycles (Fig. 16b) of gridded Southern Hemisphere sea level pressure. The years used in the composite are noted by asterisks in Table 2 and consist of six strong and six weak cases. Differences are computed as before with the strong and weak years subtracted from the previous years. In Fig. 16a the SLP differences for MJJ during the six relatively strong years show large significant (5% level) negative differences lying over and just to the south of Australia. As was seen in the station data, relatively lower SLP is present over northern Australia and to the southwest of the long-term mean axis of the SPCZ in the southwestern Pacific. Even though the gridded SLP data are considered to be unreliable north of about 20°S (Trenberth and Christy, 1985) there is agreement in sign in this area with the station data. Other studies of the northern Australian region (e.g., Nicholls et al., 1982; Nicholls, 1984a,b; Shukla and Paolino, 1983) are also consistent with this result. Significant areas of relatively lower pressure are present near southern South America and south of the southern tip of Africa. Relatively higher pressure is seen over Antarctica reaching out into the Indian Ocean southwest of Australia, the Pacific Ocean south of New Zealand, and the Atlantic Ocean southeast of South America. Conversely for the relatively weak years (Fig. 16b), the troughs in the three oceans are relatively deeper and the negative differences extend into the regions of the subtropical high pressure cells in the Indian and Pacific Oceans. Pressure is relatively higher over Australia and southwest of the SPCZ axis in the Pacific. This indicates that at the beginning of a relatively strong annual cycle during MJJ, the circumpolar trough southwest of Australia and south of New Zealand is weaker while positive differences, indicating higher pressure, are present in the regions of the subtropical highs in the Indian and Pacific Oceans. The converse is true for the weak composites. The largest and most extensive areas of significant sea level pressure differ-

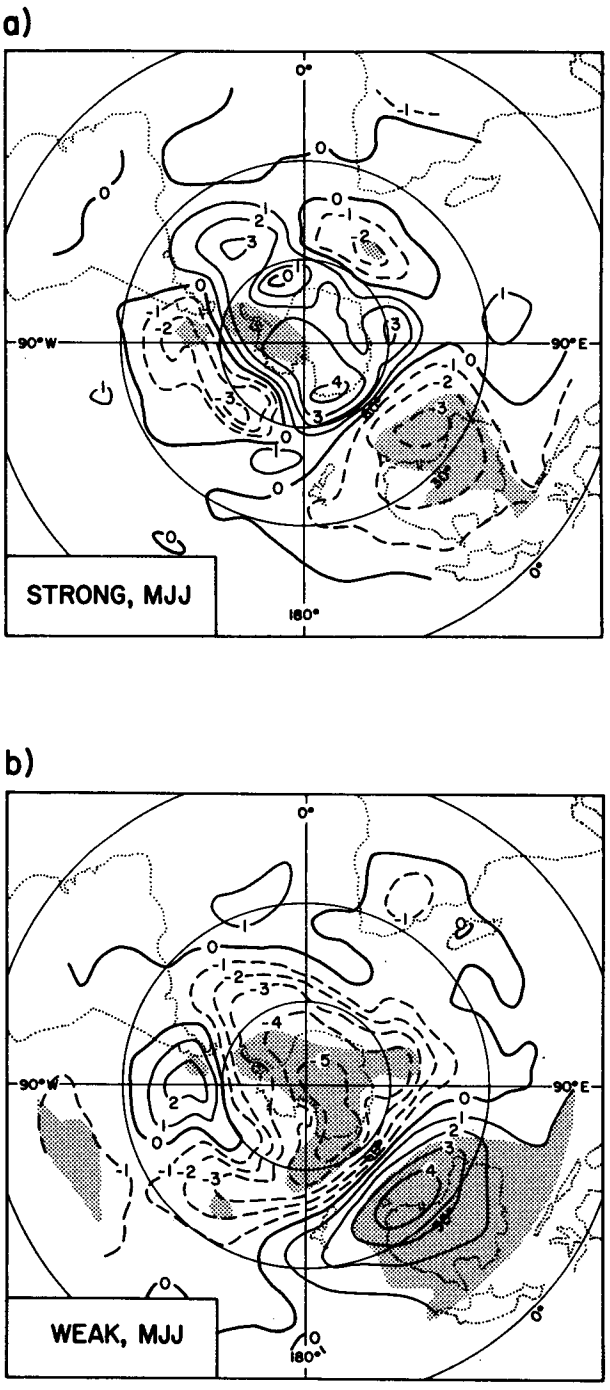


FIG. 16. Southern Hemisphere gridded sea level pressure data for (a) strong and (b) weak seasonal differences (mb), May, June, July (MJJ), minus the respective previous MJJs. Positive differences indicating higher pressure are solid contours, negative differences indicating lower pressure are dashed contours. Areas of significance at the 5% level are stippled. Years for strong and weak composites are denoted by asterisks in Table 2.

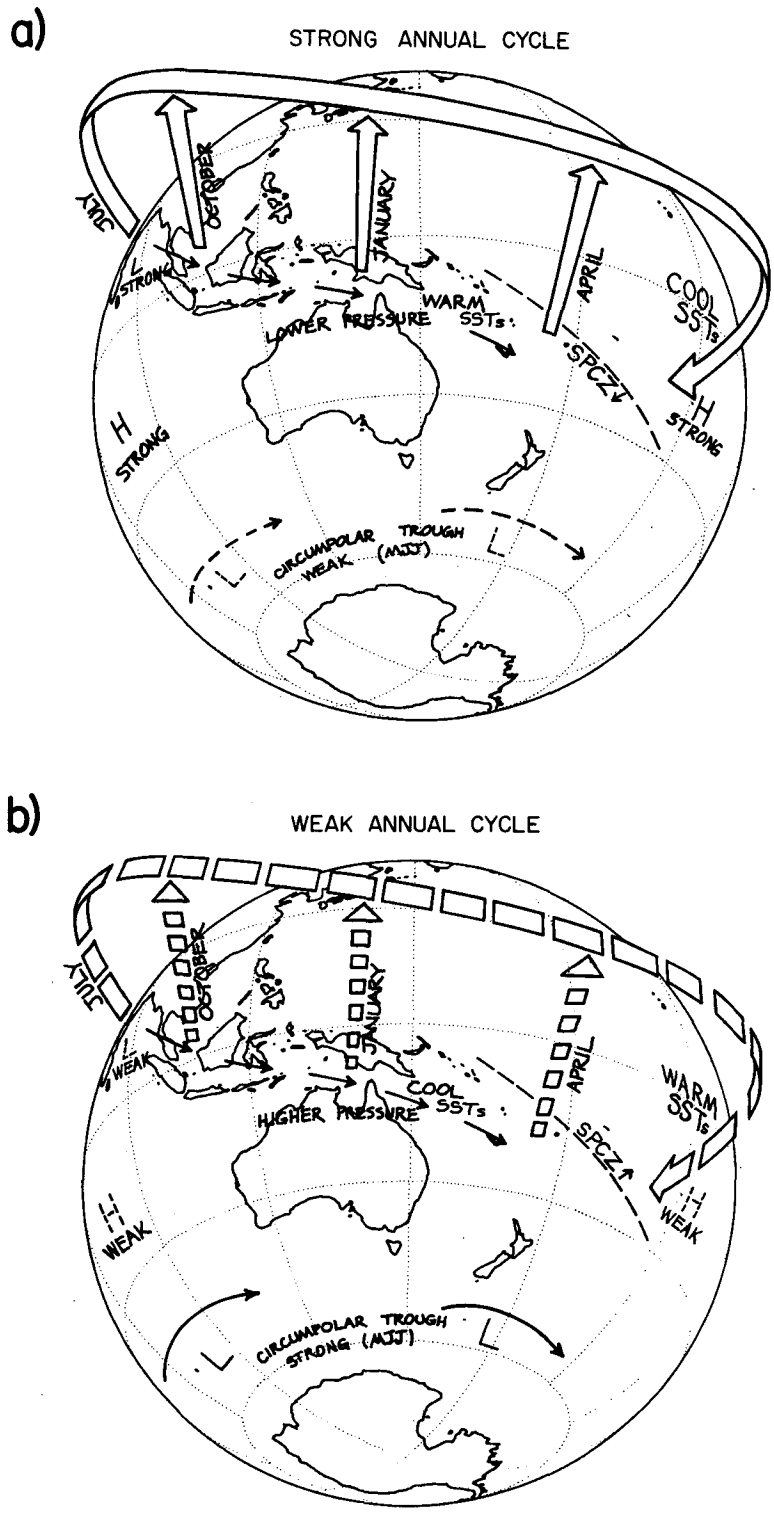


FIG. 17. Schematic diagram illustrating processes which evolve during (a) strong and (b) weak composite annual cycles. At the top, a strong annual cycle (which in the extreme is a Cold Event but occurs in other years as well) is characterized by a relatively strong Indian monsoon during Northern summer. This is associated with lower pressure, increased rainfall and warmer SSTs in the tropical regions west of the SPCZ. Consistent with the redistribution of mass by relatively stronger west–east circulations (indicated by ribbon arrows), higher pressure exists in the tropics to the east of the SPCZ along

ences are in the Australian region for both the strong and weak composites. Evolution of mid- and high-latitude circulation features involved with the circumpolar trough during Cold and Warm Events is examined further in a study in progress. Preliminary results show that as the annual cycle proceeds, the circumpolar trough subsequently strengthens during southern summer as a Cold Event (or strong annual cycle in the present context) evolves, and vice versa for a Warm Event.

## 8. Discussion and conclusions

From the preceding results, a consistent composite picture begins to emerge which describes the behavior of the dynamically coupled ocean-atmosphere system in about two thirds of the years since 1900. It involves SO-type features that continually evolve throughout the annual cycle from one year to the next as a consequence of the east–west circulations between the Indian and Pacific sectors, and the associated oceanic interaction. Relatively strong and weak years were defined from an index of Indian monsoon rainfall. Such a rainfall index was chosen to be representative of relative strength of precipitation and convection over the Indian sector in northern summer. This was deemed to be an appropriate starting point to examine the seasonal cycle because it was seen that the mean convective maximum is stronger in its southeastward traverse from northern summer to northern winter than during the northwestward return excursion in the other half of the year over the Indian–Pacific tropics. The May–June–July (MJJ) period is also thought to be important in terms of the transition to Warm Events, one of the extremes of the SO (van Loon and Shea, 1985). It also is one of the two times a year when the circumpolar trough in the SH midlatitudes is expanded farthest equatorward in the mean (van Loon, 1967). Stations in the path of the convective maximum tend to reflect the state of the east–west circulations and SST pattern throughout the annual cycle in strong and weak years. Stations to the west of the SPCZ lie in relatively lower pressure, higher SSTs and greater rainfall during much of an annual cycle running from May–April for strong years, while stations to the east lie in higher pressure, lower SSTs and less rainfall. This is more specifically true, as the annual cycle evolves, for stations just ahead of the seasonal migration of the convective maximum. That is, as a relatively strong monsoon is taking place in India, SSTs cool in the Indian Ocean in conjunction with the strong subtropical high there and associated stronger surface winds, while warmer SSTs lie to the southeast in the regions north of Australia and the SPCZ. This relationship has been suggested by Nicholls (1983). At the same time, a strong subtropical high in the Pacific is associated with low SSTs in the tropical eastern Pacific. As the seasonal cycle evolves, the convective maximum moves over warmer SSTs in the Indonesia/northern Australian regions. These warmer SSTs could be maintained in southern winter and spring by weaker seasonal easterly winds and decreased upper ocean mixing and latent heat flux as suggested by early Dutch investigators Braak and Berlage (summarized by Hackert and Hastenrath, 1986), Nicholls (1981), and Hackert and Hastenrath (1986). Larger rainfall amounts occur just prior to and at the beginning of the local rainy season in the North Australia region. A relatively strong Australian monsoon subsequently is established in conjunction with these precursor conditions (also noted, for example, by Shukla and Paolino, 1983; Nicholls et al., 1982; Nicholls, 1984a,b). SSTs north of Australia decrease as the stronger monsoon continues, possibly in response to the mechanism postulated by the previously mentioned Dutch investigators, Nicholls (1981), and Hackert and Hastenrath (1986), whereby stronger seasonal westerly surface winds during the monsoon are associated with increased upper ocean mixing and greater heat removal from the ocean via stronger latent heat flux. Strong convection then becomes established over the warmer water in the SPCZ region during late northern winter and spring. These relatively warm SSTs could be maintained in this region until the convective maximum moves into the area by mechanisms proposed by van Loon and Shea (1985) whereby relatively low pressure to the west and high pressure to the east of the SPCZ set up anomalous northerly winds and ocean

with decreased rainfall and lower SSTs. During the onset of the Indian monsoon in northern summer, the subtropical high in the Indian Ocean is strong and the circumpolar trough in the Southern Hemisphere midlatitudes is weak during May–June–July (MJJ) southwest of Australia and south of New Zealand. As the annual cycle evolves from northern summer to northern winter, the tropical convective maximum remains strong as it moves southeastward over high SSTs. As it reaches the Pacific the SPCZ is shifted to the southwest over the warm SSTs there. Strong convection and lower pressure in the SPCZ region weakens or reverses the pressure gradient to the north in the western equatorial Pacific, and erodes the strength of the South Pacific High which weakens the trade winds and leads, in some years, to the transition to a relatively weak year (b). The dynamical response of the ocean is associated with warm SSTs which appear in the equatorial eastern Pacific along with lower pressure, increased convection, and a northeastward shift of the SPCZ. The mean west–east circulation is weakened (indicated as anomalous east-to-west flow by ribbon arrows) and a weak year (which in the extreme is a Warm Event but occurs in other years as well) proceeds with conditions opposite to those in a strong year.

surface currents from warm regions in the deep tropics. Such relationships in this region between the maintenance of quasi-biennial circulation patterns and SSTs also have been addressed by Trenberth (1975). As relatively greater convection is established in the SPCZ, lower SLP there is associated with anomalous cyclonic flow to the north in the equatorial tropics. This anomalous pressure gradient would be conducive to westerly surface wind anomalies associated with the initiation of Warm Events in the extreme or, in the terminology of this paper, the transition from a relatively strong year to a relatively weak year (i.e., relatively strong Indian monsoon and suppressed convection in the eastern tropical Pacific to relatively weak Indian monsoon and enhanced convection in the eastern tropical Pacific). Such observed relationships in this region have been addressed by Newell et al. (1982). The ocean could respond in a way modeled by Philander and Seigel (1985) such that warm water begins to appear in the eastern tropical Pacific in response to the anomalous westerly surface wind stresses associated with the SLP anomalies in the western Pacific. In a somewhat more detailed scenario Gill and Rasmusson (1983) postulate that the coupled SST/surface-wind/convection interaction leads to the eastward shift of convection and warm SSTs in the equatorial Pacific. In any event, the evidence indicates that the equatorial Pacific and its interaction with surface wind anomalies is crucial during the transition from one mode to the other. Throughout the rest of the annual cycle, atmosphere–ocean coupling in the entire tropical belt over the India–Pacific region is important. In the words of Bjerknes (1969), "there is ample reason for a never-ending succession of alternating trends by air–sea interaction in the equatorial belt, but just how the turnabout between trends takes place is not yet quite clear." It would appear necessary to consider, at the very least, the entire ocean–atmosphere system in the Indian–Pacific tropics and subtropics of which the equatorial Pacific is but one, albeit major, part. Philander and Seigel (1985) summarize in this way: "El Niño clearly is a phenomenon with a considerable latitudinal extent and involves far more than the equatorial wave guide." That statement could be broadened to include the entire spectrum of circulation anomalies of which El Niño or Warm Events are one extreme manifestation.

It was seen that in roughly two thirds of the years since 1900, composites of the oscillations between the Indian and Pacific sectors exhibit some characteristics of Cold Events (often relatively strong monsoon years) or Warm Events (often relatively weak monsoon years). The extremes of the oscillation, the Warm and Cold Events, provide by far the largest signal. But the other strong and weak years, which are not Warm or Cold Event years, also show a similar seasonal evolution of composite anomalies with a much smaller amplitude. This implies a nearly biennial signal roughly every two out of three years, with the Warm and Cold Events surging to extremes in the cycle. Such relationships between a quasi-biennial signal in these regions and the SO signal recently have been investigated by Yasunari (1985).

In any case, the east–west circulations are a part of continuous pulsations of the coupled ocean–atmosphere system in the Indian and Pacific sectors. Some of the pulsations may be of the type identified by Barnett (1985) as eastward propagating signals of sea level pressure anomalies. The present results suggest that such apparent "eastward propagation" could be simply a local enhancement of the annual cycle. Gutzler and Harrison (1986) identify wind anomalies that move with the annual cycle from Southeast Asia in SON eastward into the Pacific as a Warm Event subsequently develops. The opposite pattern of wind anomalies then appears a year later and moves eastward. Taken together with the present results, these studies and others such as van Loon (1984) and van Loon and Shea (1985) indicate that modulation or, in the words of Gutzler and Harrison, "amplification/deamplification" of the mean annual cycle could produce these effects.

In the present study, it was seen that lower pressure, greater rainfall and warmer SSTs are associated with, in many cases, a local enhancement of the convective maximum. During the course of the seasonal excursion of the convective maximum to the southeast from northern summer to northern winter, higher pressure, reduced rainfall and cooler SSTs in the Pacific to the east of the SPCZ are often in evidence. If it is to be made in a consecutive year, a transition occurs in northern spring so that the following annual cycle is characterized by conditions opposite to that of the preceding annual cycle. So the pulsation continues as a continuous process with many years being characterized in a composite sense in one mode or the other, and a few occurring as extremes that have been documented as Warm and Cold Events. These composite processes are shown schematically in Fig. 17 and can be summarized as follows:

1) In the top of Fig. 17, a "strong" year (often a Cold Event in the extreme) is characterized by a relatively strong Indian monsoon which is indicative of lower pressure, and greater precipitation, convection and upward motion over the Indian region during northern summer. Lower surface pressure, warmer SSTs, and enhanced rainfall occur over the Indian sector in the tropics west of the SPCZ, with higher pressure, cooler SSTs and suppressed rainfall to the east of the SPCZ in the South Pacific. These conditions are associated with intensified mean west-to-east exchange of mass from the Indian to the Pacific sector shown schematically by the ribbon arrows in Fig. 17a. In the Southern Hemisphere mid-latitudes a weakened circumpolar trough south of New Zealand and southwest of Australia during MJJ is associated with stronger subtropical highs in the Indian and Pacific oceans.

2) As the annual cycle proceeds, the convective maximum moves south and east as it traverses south-

east Asia and northern Australia, moving over a relatively warmer ocean surface.

3) The warmer SSTs ahead of the convective maximum contribute to maintaining the strong convection as it moves eastward toward the Pacific. Relatively greater rainfall occurs just prior to or during respective rainy seasons as a local enhancement of the naturally occurring seasonal cycle of the convective maximum. As the convective maximum passes, the SSTs decrease.

4) The convective maximum reaches the SPCZ in the tropical southwest Pacific early in the calendar year. The SPCZ is displaced southwestward over the warmer SSTs there. Relatively lower pressure associated with this convection then moves further south and east into the region of the South Pacific High in April. Westerly wind anomalies in the western equatorial Pacific associated with low SLP in the SPCZ and the weakened South Pacific High contribute to the processes in the equatorial Pacific Ocean which are thought to cause warm water to form in the eastern equatorial Pacific.

5) A "weak" year (Fig. 17b, often a Warm Event in the extreme) is then characterized by warm SSTs, enhanced convection and greater precipitation in the Pacific east of the SPCZ. A weakened South Pacific High, a weak subtropical high in the Indian Ocean, higher pressure in the tropical Indian sector west of the SPCZ, and relatively less rainfall during the Indian monsoon occur in association with the weakened mean west-to-east exchange of mass. This is indicated schematically in Fig. 17b by the broken ribbon arrows. The relatively weaker convective maximum then moves from India eastward to the Pacific during the course of a "weak" annual cycle with opposite conditions than those present during a "strong" annual cycle.

The set of interactions posed here presents a coherent composite picture of processes involved with the entire ocean–atmosphere coupled system in the Indian and Pacific sectors, a region which spans nearly two thirds of the global tropics and involves the entire annual cycle. It has been suggested that by its nature, the east–west exchange of mass and the dynamic ocean interaction in these regions possesses a natural biennial tendency. Extremes of this regime, as a natural consequence of modulations of the annual cycle, could partially explain occurrences of drought and flood years in the Asian monsoon regions at one end of the east–west circulation in some years, as well as Warm and Cold Events at the other in the tropical Pacific in other years. The Southern Oscillation represents extremes of the system, but similar composite signals exist in many other years with much reduced amplitude.

These processes could be disrupted by many influences in the tropics and higher latitudes, particularly from the Northern Hemisphere which has not been considered in this paper. What remains to be explained, then, is not necessarily that there is a tendency for biennial oscillations in this system to exist in composites for many years, or that extreme manifestations of this coupled ocean–atmosphere system are evidenced by the Southern Oscillation, but what causes the extremes and why do these events not occur with more regularity? The answer to those questions may lie with stochastic forcing mechanisms emanating from either the tropics or higher latitudes. It also remains to be seen if the signals present in the composites can be discerned to any useful extent in individual years.

*Acknowledgments.* The author wishes to thank Harry van Loon, Chester Newton, Warren Washington, and Kevin Trenberth for their helpful comments and discussions over several versions of the manuscript. Thanks also to Neville Nicholls for his comments, Bruce Briegleb for supplying the OLR data, Wilbur Spangler for providing access to the Southern Hemisphere SLP grids, Dennis Shea for his help with the COADS SST data, Eileen Boettner for typing the manuscript, and Stephanie Honaski and Melanie Pappas for drafting the figures.

## REFERENCES

Allan, R. J., 1983: Monsoon and teleconnection variability over Australasia during the Southern Hemisphere summers of 1973–77. *Mon. Wea. Rev.*, **111,** 113–142.

Barnett, T. P., 1985: Variations in near-global sea level pressure. *J. Atmos. Sci.*, **42,** 478–501.

Bhalme, H. N., and S. K. Jadhav, 1984: The Southern Oscillation and its relation to the monsoon rainfall. *J. Climatol.*, **4,** 509–520.

Bjerknes, J., 1969: Atmospheric teleconnections from the equatorial Pacific. *Mon. Wea. Rev.*, **97,** 163–172.

Busalacchi, A. J., and J. J. O'Brien, 1981: Interannual variability of the equatorial Pacific in the 1960s. *J. Geophys. Res.*, **86,** 10901–10907.

Cadet, D., 1983: The monsoon over the Indian Ocean during summer 1975. Part II: Break and active monsoons. *Mon. Wea. Rev.*, **111,** 95–108.

Cane, M. A., and S. E. Zebiak, 1985: A theory of El Niño and the Southern Oscillation. *Science,* **228,** 1085–1087.

Davidson, N. E., J. L. McBride and B. J. McAvaney, 1983: The onset of the Australian monsoon during winter MONEX: Synoptic aspects. *Mon. Wea. Rev.*, **111,** 496–516.

Gill, A. E., and E. M. Rasmusson, 1983: The 1982–83 climate anomaly in the equatorial Pacific. *Nature,* **306,** 229–234.

Gordon, N. D., 1986: The Southern Oscillation and New Zealand weather. *Mon. Wea. Rev.*, **114,** 371–387.

Gruber, A., and A. F. Krueger, 1984: The status of the NOAA outgoing longwave radiation data set. *Bull. Amer. Meteor. Soc.*, **65,** 958–962.

Gutzler, D. S., and D. E. Harrison, 1986: The structure and evolution of seasonal wind anomalies over the near-equatorial eastern Indian and western Pacific Oceans. *Mon. Wea. Rev.*, (in press).

Hackert, E. C., and S. Hastenrath, 1986: Mechanisms of Java rainfall anomalies. *Mon. Wea. Rev.*, **114,** 745–757.

Harrison, D. E., 1984: The appearance of sustained equatorial surface westerlies during the 1982 Pacific Warm Event. *Science,* **224,** 1099–1102.

Heddinghaus, T. R., and A. F. Krueger, 1981: Annual and interannual variations in outgoing longwave radiation over the tropics. *Mon. Wea. Rev.*, **109,** 1208–1218.

Jaeger, L., 1976: Monatskarten des Niederschlags für die Ganze Erde. *Ber. Deutch. Wet.*, **139**(18), 38 pp.

Janowiak, J. E., A. F. Krueger, P. A. Arkin and A. Gruber, 1985: Atlas of outgoing longwave radiation derived from NOAA satellite data, NOAA Atlas No. 6, U.S. Dept. of Commerce, Silver Spring, MD, 44 pp.

Keen, R. A., 1982: The role of cross-equatorial cyclone pairs in the Southern Oscillation. *Mon. Wea. Rev.*, **110,** 1405–1416.

Khandekar, M. L., and V. R. Neralla, 1984: On the relationship between sea surface temperatures in the equatorial Pacific and the Indian monsoon rainfall. *Geophys. Res. Lett.*, **11,** 1137–1140.

Krishnamurti, T. N., 1971: Tropical east-west circulations during northern summer. *J. Atmos. Sci.*, **20,** 1342–1347.

——, and H. N. Bhalme, 1976: Oscillations of a monsoon system. Part I. Observational aspects. *J. Atmos. Sci.*, **33,** 1937–1954.

——, M. Kanamitsu, W. J. Koss and J. D. Lee, 1973: Tropical east-west circulations during the northern winter. *J. Atmos. Sci.*, **30,** 780–787.

Kuettner, J. P., and S. Unninayar, 1982: The onset mechanism of the Indian monsoon, *International Conference on the Scientific Results of the Monsoon Experiment, Extended Abstracts and Panel Session,* Denpasar, Bali, Indonesia, 26–30 Oct., 1981, WMO, Geneva, 3-25 to 3-32.

Lau, K. M., and P. H. Chan, 1983a: Short-term climate variability and atmospheric teleconnections for satellite-observed outgoing longwave radiation. Part I: Simultaneous relationships. *J. Atmos. Sci.*, **40,** 2735–2750.

——, and ——, 1983b: Short-term climate variability and atmospheric teleconnections for satellite-observed outgoing longwave radiation. Part II: Lagged correlations. *J. Atmos. Sci.*, **40,** 2751–2767.

——, C.-P. Chang and P. H. Chan, 1983: Short-term planetary-scale interactions over the tropics and midlatitudes. Part II: Winter-MONEX Period. *Mon. Wea. Rev.*, **111,** 1372–1388.

Liebmann, B., and D. L. Hartmann, 1982: Interannual variations of outgoing IR associated with tropical circulation changes during 1974–78. *J. Atmos. Sci.*, **39,** 1153–1162.

Love, G., 1985: Cross-equatorial influence of winter hemisphere subtropical cold surges. *Mon. Wea. Rev.*, **113,** 1487–1498.

Meehl, G. A., 1987: The tropics and their role in the global climate system. *Geogr. J.*, (in press).

——, and W. M. Washington, 1985: Sea surface temperatures computed by a simple ocean mixed layer coupled to an atmospheric GCM. *J. Phys. Oceanogr.*, **15,** 92–104.

——, and ——, 1986: Tropical response to increased $CO_2$ in a GCM with a simple mixed layer ocean: Similarities to an observed Pacific Warm Event. *Mon. Wea. Rev.*, **114,** 667–674.

Mooley, D. A., and B. Parthasarathy, 1983: Variability of the Indian summer monsoon and tropical circulation features. *Mon. Wea. Rev.*, **111,** 967–978.

Newell, R. E., R. Selkirk and W. Ebisuzaki, 1982: The Southern Oscillation: Sea surface temperature and wind relationships in a 100-year data set. *J. Climatol.*, **2,** 357–373.

Nicholls, N., 1979: A simple air–sea interaction model. *Quart J. Roy. Meteor. Soc.*, **105,** 93–105.

——, 1981: Air–sea interaction and the possibility of long-range weather prediction in the Indonesian archipelago. *Mon. Wea. Rev.*, **109,** 2435–2443.

——, 1983: Predicting Indian monsoon rainfall from sea-surface temperature in the Indonesia-north Australia area. *Nature,* **306,** 576–577.

——, 1984a: The Southern Oscillation and Indonesian sea surface temperature. *Mon. Wea. Rev.*, **112,** 424–432.

——, 1984b: The Southern Oscillation, sea surface temperature, and interannual fluctuations in Australian tropical cyclone activity. *J. Climatol.*, **4,** 661–670.

——, J. L. McBride and R. J. Ormerod, 1982: On predicting the onset of the Australian wet season at Darwin. *Mon. Wea. Rev.*, **110,** 14–17.

Pant, G. B., and B. Parthasarathy, 1981: Some aspects of an association between the Southern Oscillation and Indian summer monsoon. *Arch. Meteor. Geophys. Bioklim.*, **B29,** 245–252.

Parthasarathy, B., and D. A. Mooley, 1978: Some features of a long homogeneous series of Indian summer monsoon rainfall. *Mon. Wea. Rev.*, **106,** 771–781.

Philander, S. G. H., and A. D. Seigel, 1985: Simulation of El Niño of 1982–1983. *Coupled Ocean–Atmosphere Models,* Elsevier Oceanogr. Ser., **40,** Elsevier, 517–541.

Ramage, C. S., 1983: Teleconnections and the siege of time. *J. Climatol.*, **3,** 223–231.

Rasmusson, E. M., and T. H. Carpenter, 1982: Variations in tropical sea surface temperature and surface wind fields associated with the Southern Oscillation/El Niño. *Mon. Wea. Rev.*, **110,** 354–384.

——, and ——, 1983: The relationship between eastern equatorial Pacific sea surface temperatures and rainfall over India and Sri Lanka. *Mon. Wea. Rev.*, **111,** 517–528.

Reiter, E. R., 1983: Teleconnections with tropical precipitation surges. *J. Atmos. Sci.*, **40,** 1631–1647.

Sadler, J. C., 1970: *Mean Cloudiness and Gradient-Level Wind Charts over the Tropics,* U.S. Air Force Tech. Rept. 215, Vol. I. Part B, 22 pp and 48 charts.

Shukla, J., and D. A. Paolino, 1983: The Southern Oscillation and long-range forecasting of the summer monsoon rainfall over India. *Mon. Wea. Rev.*, **111,** 1830–1837.

Tanaka, M., 1981: Interannual fluctuations of the tropical monsoon circulation over the greater WMONEX area. *J. Meteor. Soc. Japan,* **59,** 825–831.

Trenberth, K. E., 1975: A quasi-biennial standing wave in the Southern Hemisphere and interrelations with sea surface temperature. *Quart. J. Roy. Meteor. Soc.*, **101,** 55–74.

——, and J. R. Christy, 1985: Global fluctuations in the distribution of atmospheric mass. *J. Geophys. Res.*, **90,** 8042–8052.

Troup, A. J., 1965: The southern oscillation. *Quart. J. Roy. Meteor. Soc.*, **91,** 490–506.

Van Loon, H., 1967: The half-yearly oscillation in middle and high southern latitudes and the coreless winter. *J. Atmos. Sci.*, **24,** 472–486.

——, 1984: The Southern Oscillation. Part III: Associations with the trades and with the trough in the westerlies of the South Pacific Ocean. *Mon. Wea. Rev.*, **112,** 947–954.

——, and R. A. Madden, 1981: The Southern Oscillation. Part I: Global associations with pressure and temperature in northern winter. *Mon. Wea. Rev.*, **109,** 1150–1162.

——, and J. C. Rogers, 1984: Interannual variations in the half-yearly cycle of pressure gradients and zonal wind at sea level on the Southern Hemisphere. *Tellus,* **36A,** 76–86.

——, and D. J. Shea, 1985: The Southern Oscillation. Part IV: The development of warm and cold events. *Mon. Wea. Rev.*, **113,** 2063–2074.

——, J. J. Taljaard, T. Sasamori, J. London, O. V. Hoyt, K. Labitzke and C. W. Newton, 1972: *Meteorology of the Southern Hemisphere. Meteor. Monogr.,* Vol. 13, Amer. Meteor. Soc., 263 pp.

Verma, R. K., K. Subramaniam and S. S. Dugam, 1984: Long-term variability of summer monsoon and climatic change. *Contributions from the Indian Institute of Tropical Meteorology,* Sci. Rep. R-041, Ramdury House, Pune, 41 pp. [ISSN 0252-1075.]

Walker, G. T., 1923: Correlation in seasonal variations of weather VIII. *Mem. Indian Meteor. Dept.*, **24,** 75–131.

——, 1924: World Weather IX. *Mem. Indian Meteor. Dept.*, **24,** 275–332.

——, and E. W. Bliss, 1930: World Weather IV. *Mem. Roy. Meteor. Soc.*, **3,** 81–95.

Washington, W. M., and G. A. Meehl, 1984: Seasonal cycle experiment on the climate sensitivity due to a doubling of $CO_2$ with an atmospheric general circulation model coupled to a simple mixed-layer ocean model. *J. Geophys. Res.*, **89,** 9475–9503.

Weickmann, K. M., G. R. Lussky and J. E. Kutzbach, 1985: Intraseasonal (30–60 day) fluctuations of outgoing longwave radiation and 250 mb streamfunction during northern winter. *Mon. Wea. Rev.*, **113,** 941–961.

Wyrtki, K., 1975: El Niño: The dynamic response of the equatorial Pacific Ocean to atmospheric forcing. *J. Phys. Oceanogr.*, **5,** 572–584.

Yasunari, T., 1985: Zonally propagating modes of the global east-west circulation associated with the Southern Oscillation. *J. Meteor. Soc. Japan,* **63,** 1013–1029.